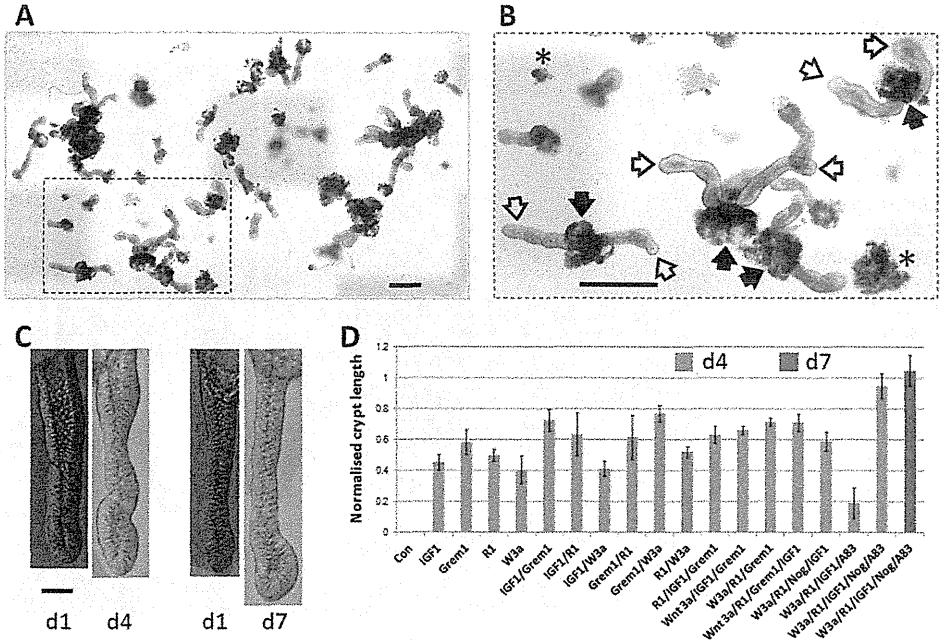

Figure 3 A combination of Wnt pathway activators and TGFβ/BMP pathway inhibitors is required for maintenance of cultured human colonic crypts ex vivo (A) Overview of human colonic crypts cultured within a Matrigel droplet under optimised conditions described in panel D; the bright field image was created by stitching together an array of 12 adjacent fields of view taken with a ×4 objective lens; scale bar=0.5 mm. (B) Enlargement of insert depicted in (A) representing a typical field of view (×4 objective lens); example crypt-base and shedding domains are denoted by open and closed arrowheads, respectively; *dead crypt fragments; scale bar=0.5 mm. (C) Example paired differential interference contrast images (×20 objective) of human colonic crypts cultured under optimised conditions for 0–4 and 0–7 days; d1=day 1, d4=day 4, d7=day 7; scale bar=100 μm. (D) Quantification of crypt length at day 4 or day 7 (with respect to the initial crypt length 4 h post-isolation, Day 0) following culture in the presence of the indicated combination of recombinant human growth factors, recombinant human BMP binding protein and/or small molecule ALK 4/5/7 inhibitor: IGF-1 (50 ng/mL), Gremlin-1 (200 ng/mL), Noggin (100 ng/mL), Wnt3A (100 ng/mL), R-Spondin-1 (500 ng/mL), A83-01 (0.5 μM); n≥6 crypts derived from N≥3 subjects.

neutralising pan-specific TGFβ antibody mimicked the effects of A83-01 (figure 7B) and a specific small molecule inhibitor of BMPR2/ALK2, DMH-1, reproduced the effect of noggin (figure 7D). In addition, activation of the BMP or TGFβ pathway abolished LGR5 expression (figure 7E).

Canonical Wnt signals combined with suppressed TGFβ/BMP pathways are permissive for tissue renewal ex vivo

The relative upward movement of crypt cells along the crypt-axis from the crypt-base was demonstrated by a classical BrdU pulse-chase approach (figure 8A). Inhibition of Wnt signalling with DKK-1 blocked the upward movement of BrdU pulse-labelled cells in the lower half of the crypt-axis into the upper-half of the crypt-axis (figure 8B). In addition to this relative migration of cells within the crypt frame of reference, absolute cell migration was also observed when crypts were cultured under suboptimal culture conditions (ie, reduced Wnt stimulation). Absolute crypt cell migration was associated with shortening of the crypt length (eg, see online supplementary figure S5), whereby the crypt-base migrated towards the crypt opening and crypt cells were shed from the surface (figure 8D). To explore the link between crypt cell proliferation and migration, crypts were cultured under conditions that imposed different levels of proliferation and were observed under time-lapse microscopy. Crypt length (figure 8Ci) and crypt cell proliferation followed a similar decreasing trend under culture conditions endowed with less proliferative potential (*cf.* figure 8Ci,Cii), but crypt cell migration rate stayed constant (figure 8Ciii). The average migration rate for crypts exhibiting a steady state length was 4.95±0.45 μm/h (n=20 crypts, N=4 patients). Cell shedding was localised to the upper crypt region as revealed by labelling of 'live' cultured crypts incubated with live/dead fluorophores, that is, calcein/propidium iodide (figure 8Di) and by immunolabelling fixed crypts for activated-caspase-3 (figure 8Dii). The accumulation of shed cells at the crypt opening was monitored in real time by observing discrete, intense bursts of red fluorescence associated with propidium iodide binding to cell nuclei following membrane rupture (figure 8Ciii and online supplementary movie S4). Thus, under these conditions, crypt cell proliferation in the lower half of the crypt is required to maintain a steady-state crypt cell population (eg, constant crypt length) by replenishing cells shed from the upper surface, but does not appear to drive (ie, mitotic pressure) crypt cell migration per se.

DISCUSSION

Intestinal tissue renewal is fundamental to long life and lifelong health. The processes by which the intestinal epithelium renews itself have been well described in the mouse, but the molecular and cellular mechanisms that govern tissue renewal in the human gut are less well understood. Central to gaining a more detailed understanding is the development of model systems for the native human intestinal epithelium. Ideally, these should recapitulate the processes of tissue renewal in health and disease. Another desirable requirement is that ex vivo human tissue models are amenable to bioimaging and functional genomic approaches. Complementary to the recent development of intestinal organoid culture systems, we have developed a culture model of near-native human colonic crypts. Presently, we have demonstrated a requirement for canonical Wnt signals and suppressed TGFβ/BMP pathways to support intestinal stem

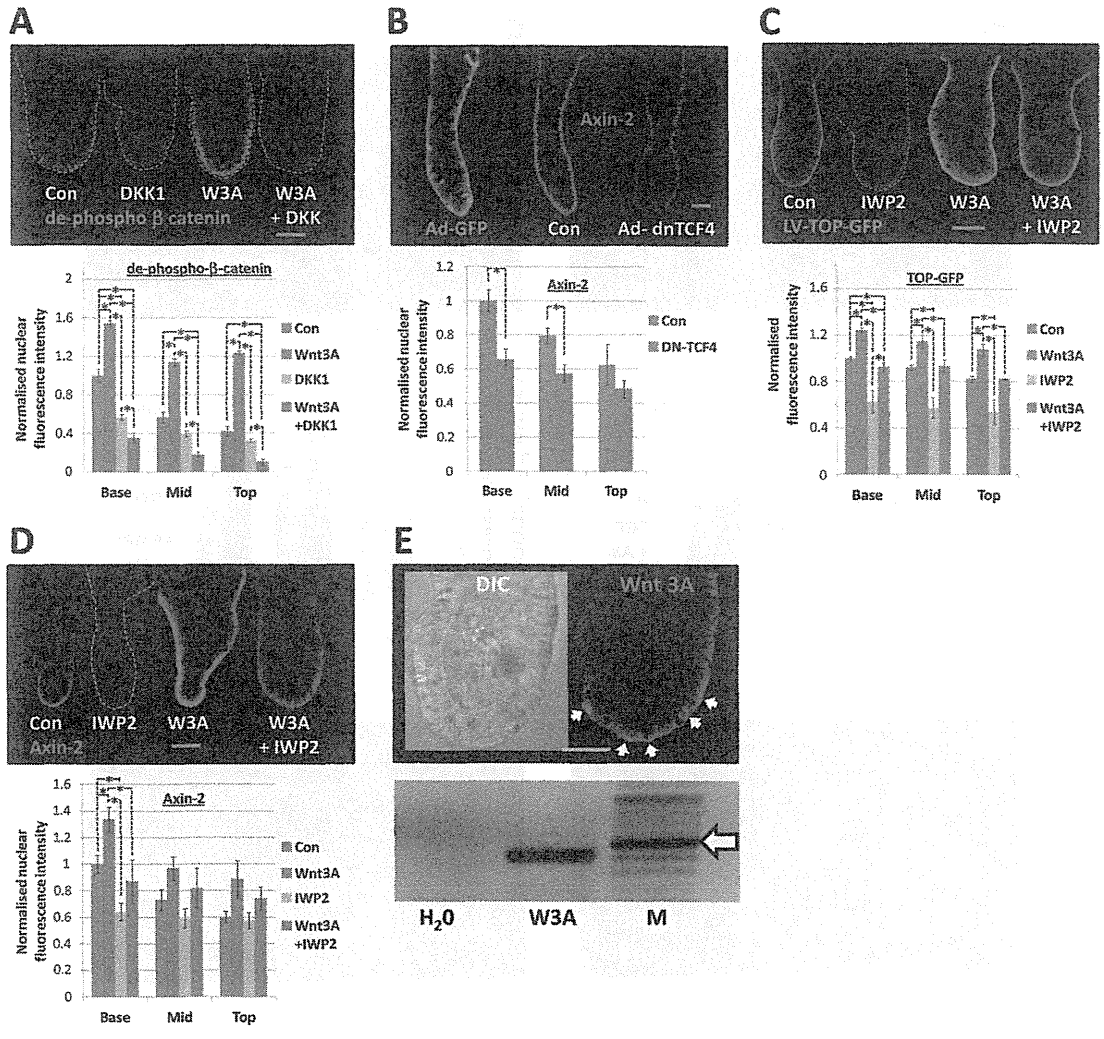

Figure 4 Exogenous and crypt-autonomous Wnt ligand promotes canonical Wnt/β catenin signals in cultured human colonic crypts. (A) Confocal images of dephospho β catenin immunolabelling following treatment with exogenous Wnt-3A (100 ng/mL, 30 min), in the presence or absence of Dikkopf-1 (DKK-1; 800 ng/mL); bar chart illustrates image analysis of nuclear immunofluorescence intensity. (B) Visualisation and analysis of nuclear Axin-2 3 days post-transduction with adenoviral GFP (Control: green Ad-GFP; red—Axin2) or dominant negative-TCF4. Effects of IWP2 (2 μM) on lentiviral (LV)-TOP-GFP expression (C) and nuclear axin-2 (D) immunofluorescence following 3 days culture. (E) Immunolabelling of human Wnt-3A (arrows indicate intense labelling basal membranes) and expression of Wnt-3A mRNA by RT-PCR using cDNA from freshly isolated human colonic crypts; expected Wnt 3A PCR product is 404 bp and the arrow denotes a 500 bp marker. All values in (A)–(D) bar charts were normalised to the control value in the crypt-base region. Control media: for A, C and D=IGF-1 (50 ng/mL)/Noggin (100 ng/mL)/R-spondin-1 (500 ng/mL); Wnt-3A (100 ng/mL) where indicated; for B=IGF-1 (50 ng/mL)/Noggin (100 ng/mL)/R-spondin-1 (500 ng/mL)/Wnt-3A (100 ng/mL). Statistical significance assessed by ANOVA followed by Tukey's post-hoc analysis; significant differences between pairs of mean values are indicated by linked dashed lines, *$p<0.01$; $n\geq4$ crypts for each experimental group and the data are representative of at least three independent experiments in each case.

cell-driven tissue renewal in the human colon. Non-repressed TGFβ/BMP signals inhibited the canonical Wnt signalling pathway, intestinal stem cell marker expression and crypt cell proliferation, while unabated crypt cell migration and shedding resulted in the appearance of drastically shortened crypts and a compromised crypt cell population.

Intestinal stem cells play a central role in tissue renewal and a strategy to label these cells in situ was imperative. Lineage tracing,[8] propagation of self-renewing intestinal organoids[27] and transplantation[22] assays have defined LGR5 as a marker of proliferative intestinal stem cells. Characterisation of the mouse small intestinal stem cell transcriptome identified a number of highly enriched genes including OLFM4,[30] which, although not expressed in the mouse colon, was also enriched in human colonic stem cells.[21 31] The current study used confocal imaging of whole-mounted intact human colonic crypts to visualise double labelling of OLFM4 protein and either LGR5 protein or LGR5-mRNA at subcellular resolution. We identified a number of $LGR5^{+}/OLFM4^{+}$ slender cells at the base of human colonic crypts, interspersed between goblet-like cells. This is reminiscent of the case for LGR5-GFP positive cells in the mouse colon.[32] A subpopulation of $LGR5^{+}/OLFM4^{+}$ cells existed that were more intensely labelled with LGR5 protein or mRNA (figure 1C,D). By analogy with sorting of single $LGR5^{GFP\text{-}Hi}$ cells from the mouse intestine[32] and $EPHB2^{Hi}$ (a surrogate marker for LGR5-positive cells) cells from the human colon,[21] it is likely that immunolabelling of $LGR5^{Hi}/OLFM4^{+}$ cells indicate the human intestinal stem cells proper and that $LGR5^{Lo}/OLFM4^{+}$ are progenitors. Indeed, OLFM4 mRNA expression has been shown to extend beyond $LGF5^{Hi}$ cells.[26 33] It is also noteworthy that recent observations of the mouse intestine

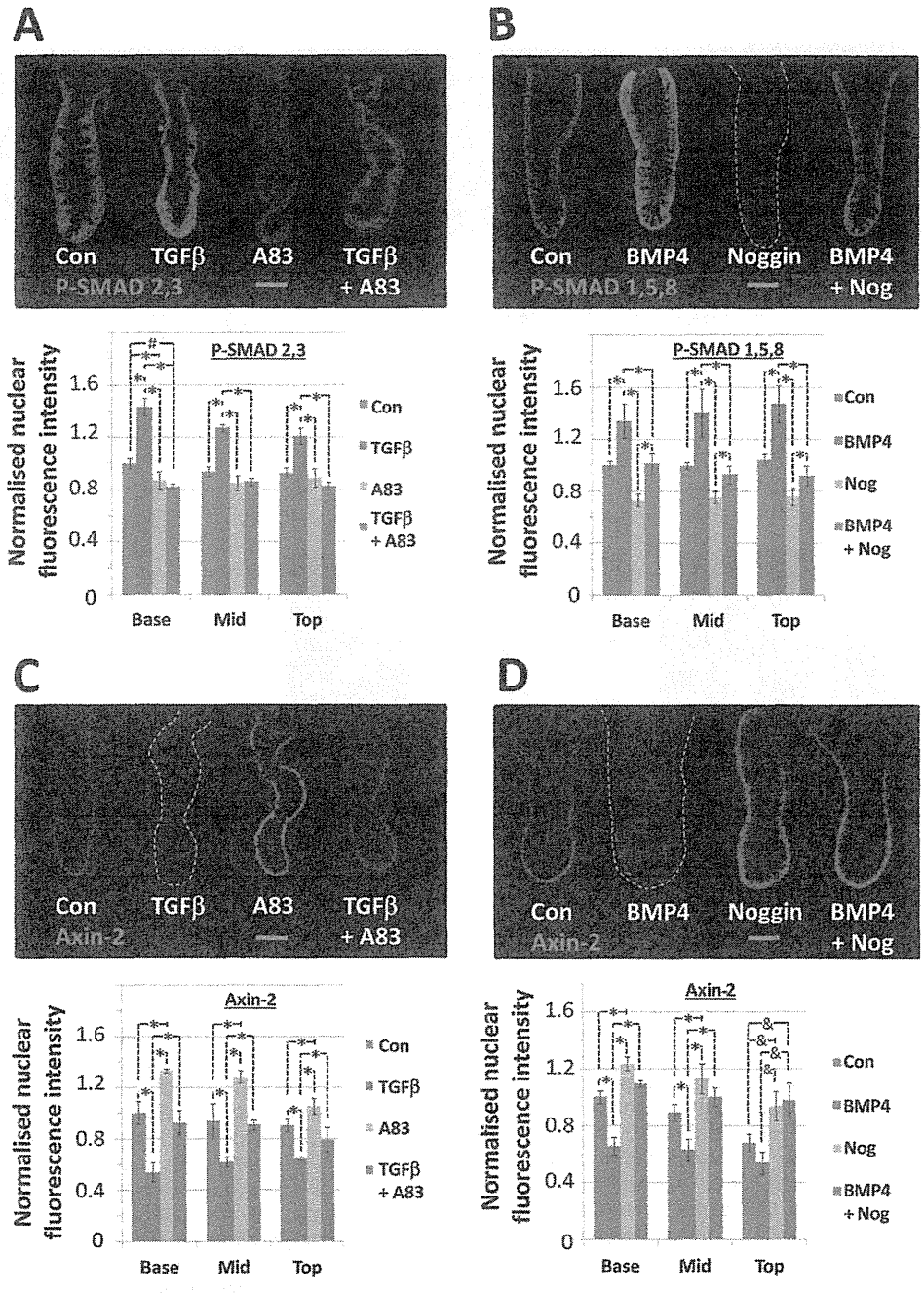

Figure 5 TGFβ and BMP pathway activation inhibits canonical Wnt signalling along the cultured human colonic crypt-axis. (A) Confocal images of phospho-SMAD2,3 immunolabelling following treatment with TGFβ (20 ng/mL, 2 days), in the presence or absence of A83-01 (0.5 μM); bar chart illustrates image analysis of nuclear immunofluorescence intensity. (B) Effects of BMP (100 ng/mL, 2 days) and/or noggin (100 ng/mL) on nuclear phospho-SMAD1,5,8 immunofluorescence intensity levels. (C) TGFβ and (D) BMP suppression of nuclear Axin-2 immunofluorescence, and rescue by pretreatment with noggin or A83-01, respectively. All values in (A–D) were normalised to the control value in the crypt-base region. Culture conditions: (A and C)—IGF-1 (50 ng/mL)/R-spondin-1 (500 ng/mL)/Wnt-3A (100 ng/mL)/Noggin(100 ng/mL) and TGFβ (20 ng/mL) and/or A83-01 (0.5 μM) where indicated; (B and D)—IGF-1 (50 ng/mL)/R-spondin-1 (500 ng/mL)/Wnt 3A (100 ng/mL)/A83-01 (0.5 μM) and BMP (100 ng/mL) and/or noggin (100 ng/mL) where indicated. Significant differences were assessed by ANOVA followed by Tukey's post-hoc analysis; significant differences between pairs of mean values are indicated by linked dashed lines; $^{\#}p<0.01$, $^{*}p<0.02$, $^{\&}p<0.05$; $n\geq4$ crypts for each experimental group and the data are representative of at least three independent experiments in each case. Scale bars=75 μm.

point to increased plasticity of crypt progenitor cells in that they can dedifferentiate into intestinal stem cells following injury.[34] In this respect, it will be fascinating to determine the precise relationship between $LGR5^{Hi}$/$OLFM4^{+}$ cells, $LGR5^{Lo}$/$OLFM4^{+}$ cells and stem cell potential following injury, and with respect to ageing and cancer risk.[35]

A functional role for morphogen gradients in conferring a crypt stem/progenitor phenotype was indicated by distinct profiles of signal pathway activation along the crypt-axis (figure 2). Substituting EGF with IGF-1 restrained the formation of multiple buds that is associated with mass expansion of intestinal stem cells in organoid culture.[20 21] These modified conditions

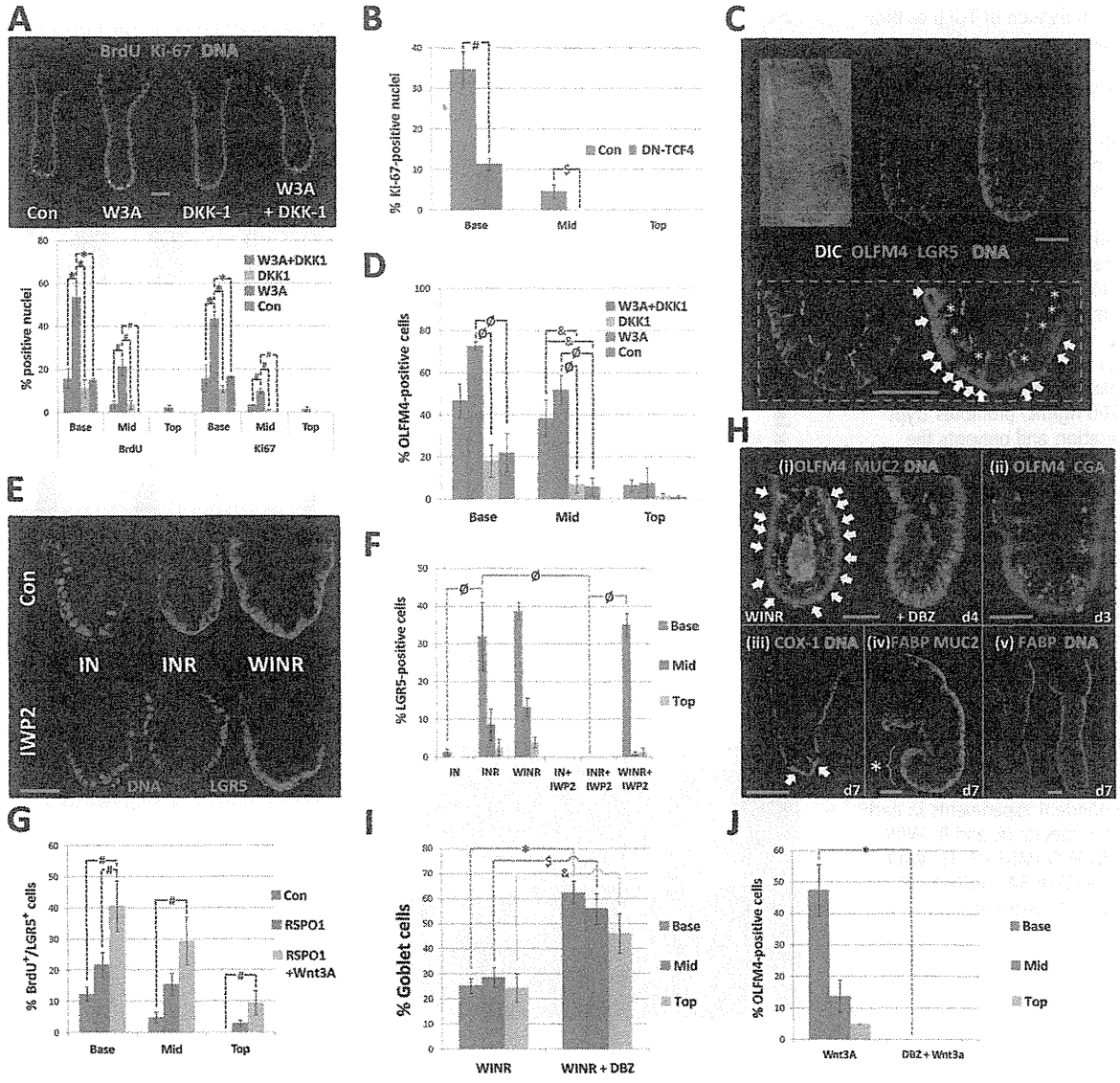

Figure 6 Canonical Wnt signals maintain cultured human colonic crypt stem/progenitor cell proliferation. (A) Effects of exogenous Wnt-3A (100 ng/mL) and/or DKK-1 (800 ng/mL) on nuclear BrdU uptake and Ki67 labelling after 3 days culture. (B) Dominant-negative TCF4 abrogates crypt cell proliferation 3 days post-transduction. (C) Coexpression of OLFM4 and LGR5 by a population of slender cells (arrowheads) interspersed between goblet-like cells (asterisk) located at the base of human colonic crypts cultured for 4 days. (D) The relative effects of Wnt-3A (100 ng/mL) and DKK-1 (800 ng/mL) on the percentage of OLFM4-positive cells following 3 days in culture. (E) Confocal images and (F) image analysis of LGR5 immunolabelling following 4 days in culture: suppression by IWP2 (2 μM) and rescue by exogeneous Wnt-3A (100 ng/mL). (G) Wnt pathway activators promote BrdU incorporation into the nuclei of LGR5-positive colonic crypt cells. (H) Immunolabelling of differentiated cell types in cultured colonic crypts: distinct labelling of cells positive for (i) MUC-2 or OLFM4 (arrows), (ii) chromogrannin A or OLFM4, and (iii) COX-1; all shown at the base of human colonic crypts; (iv, v) intense FABP1 labelling at the crypt opening (asterisk and bracket indicate crypt-base). The effects of the Notch inhibitor, DBZ (1 mM) on goblet cell number and OLFM4-positive cell number illustrated in (H) are quantified in (I and J), respectively. Significant differences were assessed by ANOVA followed by Tukey's post-hoc analysis; significant differences between pairs of mean values are indicated by linked dashed lines; *p<0.001, $p<0.002, ø p<0.02, #p<0.01, &p<0.05. Scale bars=50 μm. Control media: I=IGF-1 (50 ng/mL), N=Noggin (100 ng/mL), R=R-spondin-1 (500 ng/mL), A83-01 (0.5 μM); W3A or W=Wnt-3A (100 ng/mL), DKK-1 (Dikkopf-1; 800 ng/mL) and DBZ=dibenzazepine (1 mM) where indicated.

supported the homeostatic renewal of the crypt cell population by maintaining the hierarchy of crypt cell proliferation, migration, differentiation and shedding, while the crypt length remained relatively constant. Cultured crypts exhibited a similar $OLFM4^+/LGR5^+$ cell number and proliferative activity to that observed for native crypts. Mitotic events in human colonic crypts were very distinctive: a nucleus migrated from the basal pole to the apical pole of the cell, while the cell membrane apparently maintained contact with the basement membrane via a pedestal; following cytokinesis, the daughter nuclei returned to the apical pole (see online supplementary movies S2 and S3). All barring a few of the observed mitotic events (>1000) occurred at the apical pole with only a few noticeable events at the basal pole. A comprehensive analysis of spindle orientation is yet to be conducted. The observed crypt cell migration rate of ~5 μm/h predicts a renewal cycle of just over 3 days for a crypt of length 400 μm. Significantly, crypt cell migration continued in the relative absence of crypt cell proliferation, as has been

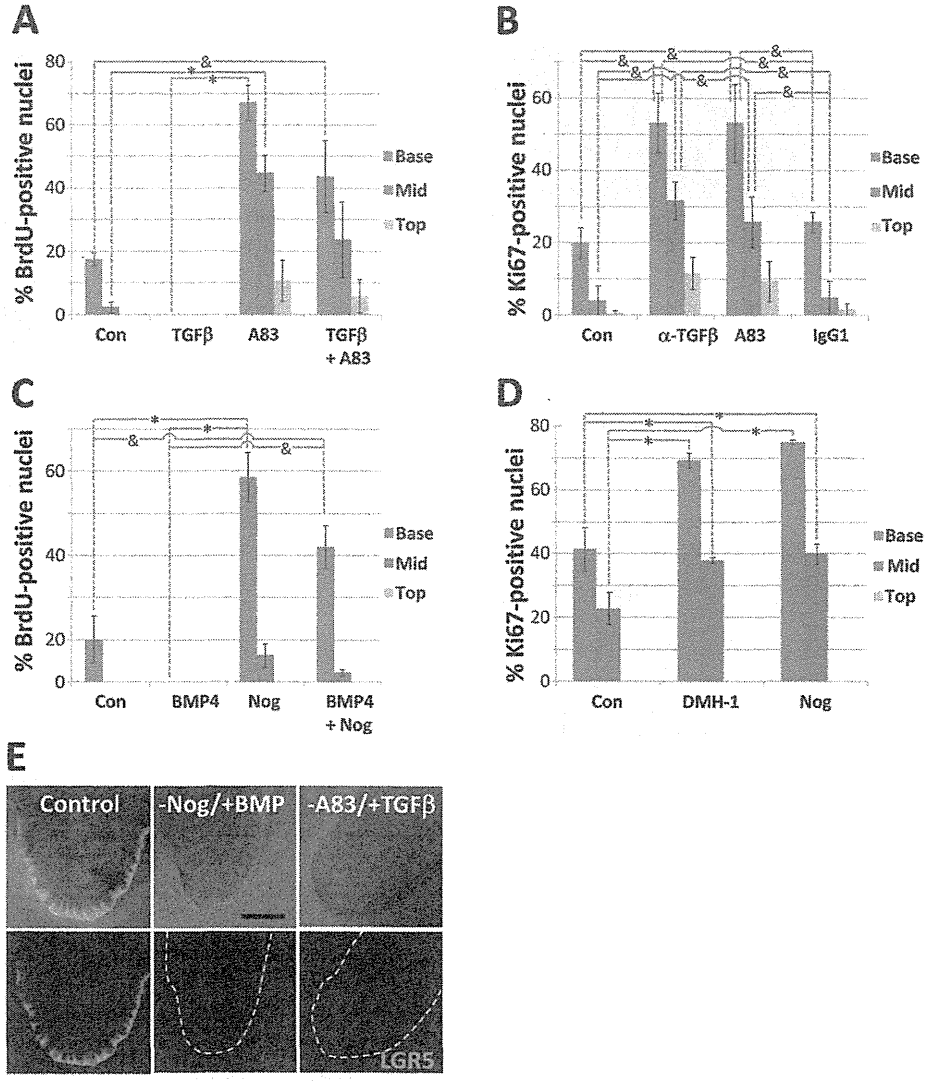

Figure 7 Activation of TGFβ or BMP pathways suppress cultured human colonic crypt stem/progenitor cell proliferation. (A) Effects of treatment with TGFβ (20 ng/mL, 2 days) and/or the ALK4/5/7 inhibitior A83-01 (0.5 μM) on nuclear incorporation of BrdU incorporation into human colonic crypt cells. (B) A pan-specific monoclonal TGFβ antibody (10 μg/mL) mimicks the effects of A83-01 (0.5 μM) on crypt cell proliferation; the irrelevant monoclonal anti-COX2 (10 μg/mL) was included as an IgG1 control. (C) BMP (100 ng/mL) abolishes human colonic crypt cell proliferation. Noggin (100 ng/mL) promotes crypt cell proliferation and prevents the inhibitory effects of BMP4. (D) The BMPR1 (ALK2/3) inhibitor DMH-1 (1 μM) mimics the stimulatory effects of noggin on crypt cell proliferation. (E) BMP pathway or TGFβ pathway activation suppress LGR5 immunolabelling. Significant differences were assessed by ANOVA followed by Tukey's post-hoc analysis; significant differences between pairs of mean values are indicated by linked dashed lines; *p<0.001, &p<0.05; n≥4 crypts for each experimental group and the data are representative of at least three independent experiments in each case. Control media: (A and B) W/I/N/R; (C and D) W/I/R/A83-01; (E) W/I/N/R/A83-01. W=Wnt 3A, I=IGF-1, 'N' or 'Nog'=noggin, R=R-spondin-1.

reported for the mouse intestine in vivo.[36] Cell shedding occurred in an organised manner and cells did not lose membrane integrity until they were extruded from the cell monolayer. Although known to stimulate colon cancer cell lines, the actions of IGF-1 on the native human colonic epithelium are not that well described.[28] IGF-1 stimulated crypt cell proliferation (not shown) and it will be informative to investigate the potential for Wnt signalling pathway transactivation.[37]

Exogenous Wnt ligand was required for human colonic crypt culture. Maintenance of a Wnt signalling gradient sustained the hierarchy of tissue renewal for at least 7 days. However, in the first few days of culture in the absence of exogenous Wnt ligand, crypts exhibited basal levels of Wnt signal activation, stem cell marker expression and cell proliferation. These traits were abolished by IWP2, an inhibitor of Wnt ligand secretion.[38] In support of crypt cell-autonomous secretion of Wnt ligand, isolated crypts expressed *Wnt 3A* mRNA and immunolabelling for Wnt 3A identified positive cells within the stem cell niche at the crypt-base. However, in contrast to mouse Paneth cells (a source of Wnt ligand for neighbouring small intestinal stem cells) mouse colonic crypts do not express Wnt ligand and would appear to be completely reliant on Wnt stimulation from subepithelial sources.[39] The present observations in human colonic crypts point to a key role for the colonic crypt Wnt signalling gradient in regulating intestinal stem cell status and tissue renewal. Wnt signalling status varies along the longitudinal gut-axis[40] and is thought to be subject to epigenetic modulation in relation to ageing and cancer.[41 42] Disruption of the colonic crypt Wnt signalling gradient would be expected to impact on crypt renewal homeostasis and influence disease risk. In fact, higher concentrations of Wnt 3A ligand caused mass expansion of intestinal stem/progenitor cells along the crypt-axis (not shown) and we are currently investigating the consequences to crypt cell renewal and the relevance to disease onset.

The colonic crypt signalling Wnt gradient is subject to influence by other morphogens. Cross-talk between Wnt and TGFβ/BMP pathways has been documented in the mouse intestine in vivo[14 15 43] and ex vivo[44] via transcriptional[15] and non-transcriptional[14] regulation of β catenin. Here we demonstrate that TGFβ/BMP downregulates Wnt signals in human colonic crypts and suppresses stem cell marker and stem/progenitor cell proliferation as a consequence. In a more spatially defined context, it has been demonstrated in the mouse that de novo crypt regeneration following injury is dependent on the confined induction of TGFβ expression. The resulting localised inhibition of crypt cell proliferation, in combination with maintained Wnt signalling in the vicinity, throws the epithelium into nascent crypt domains.[26]

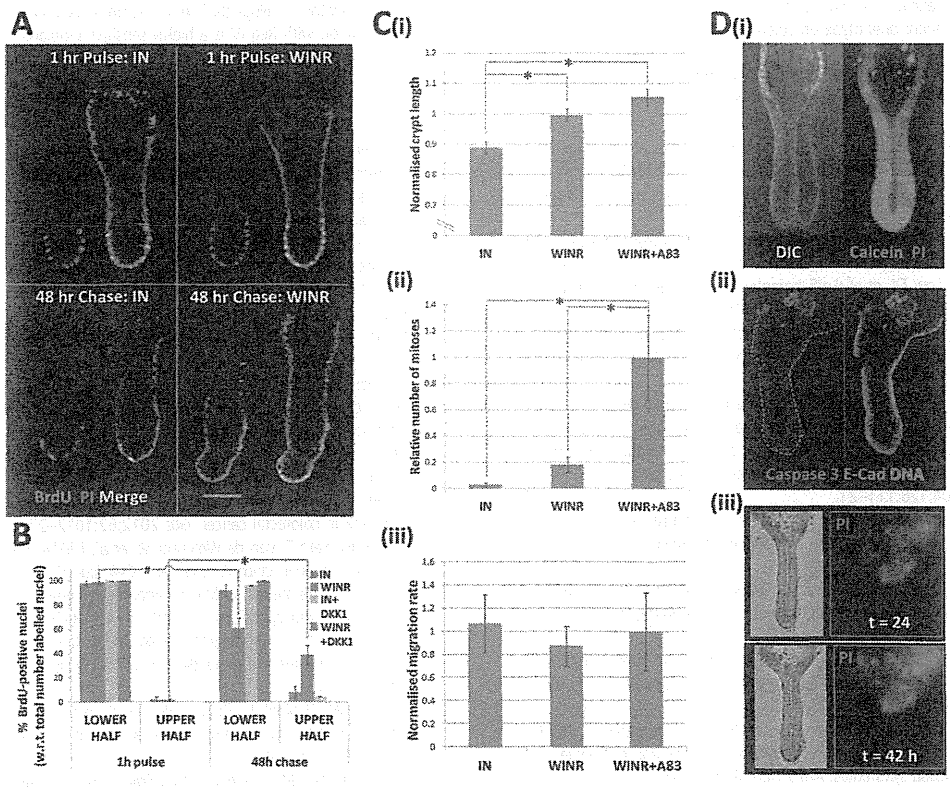

Figure 8 Crypt cell migration and shedding complete tissue renewal ex vivo. (A) A BrdU pulse-chase experiment demonstrating the relative upward migration of cells from the crypt-base along the crypt-axis in the absence (IGF-1, 50 ng/mL and Noggin, 100 ng/mL) or presence of Wnt stimulation (Wnt-3A, 100 ng/mL and R-spondin-1, 500 ng/mL); for each condition, images are shown 1 h following the BrdU pulse and 2 days after the 'cold' chase. (B) Analysis of BrdU pulse-chase images illustrating the respective decrease and increase in BrdU-positive crypt cells in the lower and upper half of the crypt in the presence of Wnt stimulation. (C) Analysis of time-lapse data acquired during days 2–3 in culture under different degrees of Wnt and TGFβ signalling pathway activation; relative changes in crypt length (Ci) and crypt cell mitoses (Cii) versus constant crypt cell migration (Ciii) are illustrated. (Di) hierarchy of calcein-labelled live cells and propidium iodide (PI)-positive dead cells; (Dii) cells at the crypt opening are positive for activated caspase 3 and (Diii) the number of PI-positive shed cells increases over time in culture (see online supplementary movie S4). Significant differences were assessed by ANOVA followed by Tukey's post-hoc analysis; significant differences between pairs of mean values are indicated by linked dashed lines; *p<0.01. W=Wnt 3A, I=IGF-1, N=noggin, R=R-spondin-1, DKK-1=dikkopf-1.

In summary, we have developed a near-native human colonic crypt culture model. The functional interaction between morphogens and their relative influence of stem cell-driven tissue renewal reinforces the importance of the canonical Wnt signalling pathway. Future investigation of the modulators that establish morphogen gradients along the crypt-axis[16] and their influence on the efficiency of intestinal tissue renewal in health and disease promises novel insights into disease risk and prevention. The native colonic crypt model can also be used to investigate numerous other aspects of (patho)physiology including: membrane transport, microbial-epithelial interactions, mesenchymal-epithelial cell interactions, pharmacology and toxicology, in homeostasis and disease.

Correction notice This article has been updated since it was published Online First. The Open Access statement has been updated.

Acknowledgements The authors wish to thank Paul Thomas for bioimaging expertise, Andrew Loveday for technical assistance, Mohammad Abu-Elmagd for advice about in situ hybridisation, members of the Clark and Riley laboratories for quantitative reverse transcriptase polymerase chain reaction advice, Richard Evans-Gowing for expertise with H&E staining, and all the staff in the Gastroenterology Department and operating theatres at the Norfolk and Norwich University Hospital.

Contributors Data acquisition/analysis: AR, NW, AP, EM, AS, LB, AE-H, CK, AM, NO, WY. Material support: ML, CS, WS, RW, KS, RT, CJ, JH, SK, NO, WY. Study design: MRW, AR, AP, AM. Manuscript revision: All authors. Funding: MRW, AM, AS, ML. Paper authorship: MRW.

Funding The work was supported by BBSRC (BB/F015690/1, BB/D018196/1), the Boston Leukaemia and Cancer Research Fund, the Big C Appeal, the Humane Research Trust, and the John and Pamela Salter Trust.

Competing interests None.

Ethics approval East of England National Research Ethics Committee.

Provenance and peer review Not commissioned; externally peer reviewed.

Data sharing statement Unpublished data on crypt viability after 4 days, use of the alternative ALK inhibitor SB431542, suppression of LGR5-mRNA by DKK-1, IGF-1-stimulated crypt cell proliferation are available on request to the corresponding author.

REFERENCES

1 Snippert HJ, van der Flier LG, Sato T, *et al.* Intestinal crypt homeostasis results from neutral competition between symmetrically dividing Lgr5 stem cells. *Cell* 2010;143:134–44.
2 Lopez-Garcia C, Klein AM, Simons BD, *et al.* Intestinal stem cell replacement follows a pattern of neutral drift. *Science* 2010;330:822–5.
3 Scoville DH, Sato T, He XC, *et al.* Current view: intestinal stem cells and signaling. *Gastroenterology* 2008;134:849–64.
4 van der Flier LG, Clevers H. Stem cells, self-renewal, and differentiation in the intestinal epithelium. *Annu Rev Physiol* 2009;71:241–60.

5 van de Wetering M, Sancho E, Verweij C, *et al*. The beta-catenin/TCF-4 complex imposes a crypt progenitor phenotype on colorectal cancer cells. *Cell* 2002;111:241–50.
6 Kuhnert F, Davis CR, Wang HT, *et al*. Essential requirement for Wnt signaling in proliferation of adult small intestine and colon revealed by adenoviral expression of Dickkopf-1. *Proc Natl Acad Sci USA* 2004;101:266–71.
7 Pinto D, Gregorieff A, Begthel H, *et al*. Canonical Wnt signals are essential for homeostasis of the intestinal epithelium. *Genes Dev* 2003;17:1709–13.
8 Barker N, van Es JH, Kuipers J, *et al*. Identification of stem cells in small intestine and colon by marker gene Lgr5. *Nature* 2007;449:1003–7.
9 Zhao J, de Vera J, Narushima S, *et al*. R-spondin1, a novel intestinotrophic mitogen, ameliorates experimental colitis in mice. *Gastroenterology* 2007;132:1331–43.
10 de Lau W, Barker N, Low TY, *et al*. Lgr5 homologues associate with Wnt receptors and mediate R-spondin signalling. *Nature* 2011;476:293–7.
11 Carmon KS, Gong X, Lin Q, *et al*. R-spondins function as ligands of the orphan receptors LGR4 and LGR5 to regulate Wnt/beta-catenin signaling. *Proc Natl Acad Sci USA* 2011;108:11452–7.
12 Haramis AP, Begthel H, van den Born M, *et al*. De novo crypt formation and juvenile polyposis on BMP inhibition in mouse intestine. *Science* 2004;303:1684–6.
13 Hardwick JC, Van Den Brink GR, Bleuming SA, *et al*. Bone morphogenetic protein 2 is expressed by, and acts upon, mature epithelial cells in the colon. *Gastroenterology* 2004;126:111–21.
14 He XC, Zhang J, Tong WG, *et al*. BMP signaling inhibits intestinal stem cell self-renewal through suppression of Wnt-beta-catenin signaling. *Nat Genet* 2004;36:1117–21.
15 Freeman TJ, Smith JJ, Chen X, *et al*. Smad4-mediated signaling inhibits intestinal neoplasia by inhibiting expression of beta-catenin. *Gastroenterology* 2012;142:562–71 e2.
16 Kosinski C, Li VS, Chan AS, *et al*. Gene expression patterns of human colon tops and basal crypts and BMP antagonists as intestinal stem cell niche factors. *Proc Natl Acad Sci USA* 2007;104:15418–23.
17 Zhou XP, Woodford-Richens K, Lehtonen R, *et al*. Germline mutations in BMPR1A/ALK3 cause a subset of cases of juvenile polyposis syndrome and of Cowden and Bannayan-Riley-Ruvalcaba syndromes. *Am J Hum Genet* 2001;69:704–11.
18 Howe JR, Roth S, Ringold JC, *et al*. Mutations in the SMAD4/DPC4 gene in juvenile polyposis. *Science* 1998;280:1086–8.
19 Howe JR, Bair JL, Sayed MG, *et al*. Germline mutations of the gene encoding bone morphogenetic protein receptor 1A in juvenile polyposis. *Nat Genet* 2001;28:184–7.
20 Sato T, Stange DE, Ferrante M, *et al*. Long-term expansion of epithelial organoids from human colon, adenoma, adenocarcinoma, and Barrett's epithelium. *Gastroenterology* 2011;141:1762–72.
21 Jung P, Sato T, Merlos-Suarez A, *et al*. Isolation and in vitro expansion of human colonic stem cells. *Nat Med* 2011;17:1225–7.
22 Yui S, Nakamura T, Sato T, *et al*. Functional engraftment of colon epithelium expanded in vitro from a single adult Lgr5(+) stem cell. *Nat Med* 2012;18:618–23.
23 Reynolds A, Parris A, Evans LA, *et al*. Dynamic and differential regulation of NKCC1 by calcium and cAMP in the native human colonic epithelium. *J Physiol* 2007;582:507–24.
24 Lindqvist S, Hernon J, Sharp P, *et al*. The colon-selective spasmolytic otilonium bromide inhibits muscarinic M(3) receptor-coupled calcium signals in isolated human colonic crypts. *Br J Pharmacol* 2002;137:1134–42.
25 Oue N, Sentani K, Noguchi T, *et al*. Serum olfactomedin 4 (GW112, hGC-1) in combination with Reg IV is a highly sensitive biomarker for gastric cancer patients. *Int J Cancer* 2009;125:2383–92.
26 Miyoshi H, Ajima R, Luo CT, *et al*. Wnt5a potentiates TGF-beta signaling to promote colonic crypt regeneration after tissue injury. *Science* 2012;338:108–13.
27 Sato T, Vries RG, Snippert HJ, *et al*. Single Lgr5 stem cells build crypt-villus structures in vitro without a mesenchymal niche. *Nature* 2009;459:262–5.
28 Simmons JG, Ling Y, Wilkins H, *et al*. Cell-specific effects of insulin receptor substrate-1 deficiency on normal and IGF-I-mediated colon growth. *Am J Physiol Gastrointest Liver Physiol* 2007;293:G995–1003.
29 VanDussen KL, Carulli AJ, Keeley TM, *et al*. Notch signaling modulates proliferation and differentiation of intestinal crypt base columnar stem cells. *Development* 2012;139:488–97.
30 Munoz J, Stange DE, Schepers AG, *et al*. The Lgr5 intestinal stem cell signature: robust expression of proposed quiescent '+4' cell markers. *EMBO J* 2012;31:3079–91.
31 van der Flier LG, Haegebarth A, Stange DE, *et al*. OLFM4 is a robust marker for stem cells in human intestine and marks a subset of colorectal cancer cells. *Gastroenterology* 2009;137:15–17.
32 Sato T, van Es JH, Snippert HJ, *et al*. Paneth cells constitute the niche for Lgr5 stem cells in intestinal crypts. *Nature* 2011;469:415–18.
33 Ziskin JL, Dunlap D, Yaylaoglu M, *et al*. In situ validation of an intestinal stem cell signature in colorectal cancer. *Gut* 2012;62:1012–23.
34 van Es JH, Sato T, van de Wetering M, *et al*. Dll1(+) secretory progenitor cells revert to stem cells upon crypt damage. *Nat Cell Biol* 2012;14:1099–104.
35 Medema JP, Vermeulen L. Microenvironmental regulation of stem cells in intestinal homeostasis and cancer. *Nature* 2011;474:318–26.
36 Kaur P, Potten CS. Cell migration velocities in the crypts of the small intestine after cytotoxic insult are not dependent on mitotic activity. *Cell Tissue Kinet* 1986;19:601–10.
37 Playford MP, Bicknell D, Bodmer WF, *et al*. Insulin-like growth factor 1 regulates the location, stability, and transcriptional activity of beta-catenin. *Proc Natl Acad Sci U S A* 2000;97:12103–8.
38 Chen B, Dodge ME, Tang W, *et al*. Small molecule-mediated disruption of Wnt-dependent signaling in tissue regeneration and cancer. *Nat Chem Biol* 2009;5:100–7.
39 Farin HF, Van Es JH, Clevers H. Redundant Sources of Wnt Regulate Intestinal Stem Cells and Promote Formation of Paneth Cells. *Gastroenterology* 2012;143:1518–29.
40 Leedham SJ, Rodenas-Cuadrado P, Howarth K, *et al*. A basal gradient of Wnt and stem-cell number influences regional tumour distribution in human and mouse intestinal tracts. *Gut* 2012;62:83–93.
41 Suzuki H, Watkins DN, Jair KW, *et al*. Epigenetic inactivation of SFRP genes allows constitutive WNT signaling in colorectal cancer. *Nat Genet* 2004;36:417–22.
42 Belshaw NJ, Pal N, Tapp HS, *et al*. Patterns of DNA methylation in individual colonic crypts reveal aging and cancer-related field defects in the morphologically normal mucosa. *Carcinogenesis* 2010;31:1158–63.
43 Furukawa K, Sato T, Katsuno T, *et al*. Smad3 contributes to positioning of proliferating cells in colonic crypts by inducing EphB receptor protein expression. *Biochem Biophys Res Commun* 2011;405:521–6.
44 Farrall AL, Riemer P, Leushacke M, *et al*. Wnt and BMP signals control intestinal adenoma cell fates. *Int J Cancer* 2012;131:2242–52.

Oncogene (2013), 1–9

www.nature.com/onc

ORIGINAL ARTICLE

Signal peptidase complex 18, encoded by SEC11A, contributes to progression via TGF-α secretion in gastric cancer

N Oue[1], Y Naito[1], T Hayashi[1], M Takigahira[2], A Kawano-Nagatsuma[3], K Sentani[1], N Sakamoto[1], H Zarni Oo[1], N Uraoka[1], K Yanagihara[4], A Ochiai[3], H Sasaki[5] and W Yasui[1]

We built an in-house oligonucleotide array on which 394 genes were selected based on our Serial Analysis of Gene Expression (SAGE) data and previously reported array data and listed several genes related to cancer progression. Among these, we focused on *SEC11A*, which encodes the SPC18 protein. *SEC11A* mRNA expression was measured by quantitative reverse transcription–polymerase chain reaction (qRT–PCR) in gastric cancer (GC) tissue samples. Expression and distribution of SPC18 protein were investigated by immunohistochemical analysis in two independent GC cohorts (Hiroshima cohort, $n=99$ and Chiba cohort, $n=989$). To determine the effect of SPC18 on cell viability and invasiveness *in vitro*, MTT and Boyden chamber invasion assays were performed. To evaluate the influence of SPC18 on cell growth *in vivo*, GC cells were injected into severe combined immunodeficiency mice. Levels of TGF-α and EGF in media from the GC cells were measured by enzyme-linked immunosorbent assay (ELISA). Studies in human tissue revealed overexpression of *SEC11A* mRNA in 40% of 42 GC samples by qRT–PCR. Immunohistochemical analysis of SPC18 revealed that 26 and 20% of GC cases were SPC18-positive in the Hiroshima and Chiba cohorts, respectively. In both cohorts, the Kaplan–Meier analysis showed poorer survival in SPC18-positive GC cases than in SPC18-negative GC cases. Forced expression of SPC18 activates GC cell growth *in vitro* and *in vivo*. The levels of TGF-α in culture media from GC cells were reduced by knockdown of SPC18. These results indicate that SPC18 contributes to malignant progression through promotion of TGF-α secretion in GC.

Oncogene advance online publication, 2 September 2013; doi:10.1038/onc.2013.364

Keywords: SPC18; SEC11A; signal peptidase complex; prognosis; gastric cancer

INTRODUCTION

Gastric cancer (GC) is one of the most common human cancers. Better knowledge of the changes in gene expression that occur during gastric carcinogenesis may lead to improvements in diagnosis, treatment and prevention of GC.[1] We previously performed Serial Analysis of Gene Expression (SAGE) on four primary GC tissues and identified several genes whose expression was either up- or downregulated in GC.[2,3] Of these genes, *regenerating islet-derived family, member 4* (*REG4*, which encodes Reg IV) and *olfactomedin4* (*OLFM4*, also known as *GW112* or *hGC-1*) were found to encode secreted proteins and serve as high sensitive serum markers for GC.[4,5] However, expression of many genes remained unconfirmed, and their role in GC remains unclear.

In the present study, we built an in-house oligonucleotide array, on which 394 genes were selected based on our SAGE data and previously reported array data, in order to identify the genes of most relevance to gastric carcinogenesis. To build the array, first, 164 genes found to be upregulated or downregulated in GC were chosen based on our SAGE data.[2] Then, 120 genes related to GC progression or prognosis, and 110 genes related to chemosensitivity, were selected based on previous reports.[6–9] Several genes associated with GC progression were identified using our array. Among these genes, the *SEC11A* was our focus, because it is frequently overexpressed in GC. *SEC11A* encodes the SPC18 protein, which is one of the subunits of the signal peptidase complex (SPC). Most secretory proteins contain amino terminal- or internal signal peptides that direct their sorting to the endoplasmic reticulum (ER).[10] From the ER, proteins are transported to either the extracellular space or the plasma membrane through the ER–Golgi secretory pathway. The ER signal peptides are then cleaved by the SPC. It has been reported that SPC purified from canine microsomes has five distinct subunits.[11] Two of these subunits, SPC18 and SPC21, are presumed to have catalytic activity.[12] It is possible that increased activity of SPC caused by SPC18 protein overexpression could induce secretion of several kinds of growth factors; however, the expression and function of SPC proteins including SPC18 have not been investigated in human cancers.

In this study, we analyzed the expression and distribution of SPC18 in human GC by immunohistochemical analysis and examined the relationship between SPC18 staining and clinicopathologic characteristics. We show first that SPC18 can increase GC cell viability *in vitro* and *in vivo*. Second, we show that knockdown of SPC18 by RNA interference (RNAi) inhibits transforming growth factor (TGF)-α secretion in GC cells. It has been reported that treatment with TGF-α induces expression of matrix metalloproteinase (MMP)-2, MMP-7 and

[1]Department of Molecular Pathology, Hiroshima University Institute of Biomedical and Health Sciences, Hiroshima, Japan; [2]Investigative Treatment Division, Research Center for Innovative Oncology, National Cancer Center Hospital East, Kashiwa, Japan; [3]Pathology Division, and Research Center for Innovative Oncology, National Cancer Center Hospital East, Kashiwa, Japan; [4]Division of Translational Research, Research Center for Innovative Oncology, National Cancer Center Hospital East, Kashiwa, Japan and [5]Division of Genetics, National Cancer Center Research Institute, Tokyo, Japan. Correspondence: Professor W Yasui, Department of Molecular Pathology, Hiroshima University Institute of Biomedical and Health Sciences, 1-2-3 Kasumi, Minami-ku, Hiroshima 734-8551, Japan.
E-mail: wyasui@hiroshima-u.ac.jp
Received 5 March 2013; revised 4 July 2013; accepted 16 July 2013

urokinase-type plasminogen activator, which activates cancer cell invasion.[13]

RESULTS

Gene expression analysis by in-house oligonucleotide array

The in-house oligonucleotide array was used to analyze a series of 25 GC tissue samples and their corresponding non-neoplastic mucosa samples. We found six genes whose expression was significantly higher in GC at stage III/IV than in GC at stage I/II, and five genes whose expression was significantly lower in GC at stage III/IV than in GC at stage I/II (Table 1). To identify ideal biomarkers and therapeutic targets for GC, we focused on genes whose expression was higher in late-stage (stage III/IV) GC samples than those in early-stage (stage I/II) GC samples. Among these genes, expression of *MMP-7*, which encodes MMP-7 (matrilysin), was statistically the most strongly upregulated in late stage GC cases. This is consistent with previous reports that high *MMP-7* expression is associated with invasion and metastasis of GC.[14] The gene with the second-highest upregulation was *SEC11A*. *SEC11A* encodes the SPC18 protein, which is an ER signal peptidase enzyme located on the ER membrane that cleaves signal peptides from precursor proteins following their transport out of the cytoplasmic space.[10] SPC consists of SPC12, SPC18, SPC21, SPC22/23 and SPC25; of these proteins, SPC18 and SPC21 are presumed to have catalytic activity based on their homology to characterized signal peptidases.[12] It is well known that several growth factors, such as TGF-α and epidermal growth factor (EGF), have an important role in GC progression. It is possible that increased SPC activity in GC caused by SPC18 upregulation could induce the secretion of several growth factors, such as TGF-α or EGF; however, to the best of our knowledge, expression of SPC18 in human cancers including GC has not yet been studied. Therefore, investigations into *SEC11A* expression in GC tissue may yield novel and informative data in the context of regulation of GC progression.

Although some of the genes on the in-house oligonucleotide array includes genes selected based on previously reported data, inconsistent results were obtained. For example, our in-house oligonucleotide array includes *TERT* gene because we previously reported that overexpression of *TERT* mRNA is found in 90% of GC cases.[15] However, of 25 GC cases analyzed by our in-house oligonucleotide array, only two GC cases showed overexpression (GC/corresponding non-neoplastic mucosa ratio > 2) of *TERT* mRNA. Therefore, we conclude that sensitivity of our in-house oligonucleotide array is low, and measurement of mRNA expression levels by qRT–PCR is required. Although our in-house oligonucleotide array showed a marginal 1.33-fold increase in *SEC11A*, we decided to investigate *SEC11A* expression in GC tissue.

Table 1. Genes associated with tumor stage, identified by in-house oligonucleotide array

Gene symbol	*mRNA expression median (range)*		P-*value*[a]
	Stage I/II	*Stage III/IV*	
Upregulated genes in stage III/IV GC in comparison with stage I/II GC			
MMP7	1.03 (0.82–1.40)	1.32 (1.03–2.74)	0.016
SEC11A	1.01 (0.86–1.47)	1.34 (0.89–3.21)	0.028
TDGF1	0.90 (0.73–1.30)	1.26 (0.70–1.65)	0.032
DDOST	0.86 (0.48–1.46)	1.19 (0.61–2.39)	0.040
NDUFB7	1.15 (0.82–1.74)	1.45 (1.00–2.38)	0.044
SUPT4H1	1.04 (0.63–1.94)	1.40 (0.91–3.00)	0.049
Downregulated genes in stage III/IV GC in comparison with stage I/II GC			
CRELD1	0.92 (0.77–1.50)	0.76 (0.43–1.21)	0.023
AREG	1.07 (0.73–1.34)	0.89 (0.60–1.69)	0.024
HDAC2	1.02 (0.50–1.40)	0.56 (0.41–1.88)	0.026
CDC25B	0.94 (0.49–1.29)	0.63 (0.45–1.14)	0.035
PLG	1.04 (0.66–1.53)	0.70 (0.51–1.34)	0.042

[a]Mann–Whitney *U*-test.

mRNA expression of *SEC11A* in GC tissue and non-neoplastic tissue samples

We next investigated the expression of *SEC11A* in nine GC tissue samples and 12 types of normal tissue samples by quantitative reverse transcription–polymerase chain reaction (qRT-PCR) (Figure 1a). Overexpression (GC/normal stomach ratio > 2) of *SEC11A* was observed in 4 (44%) of 9 GC cases. Among the 12 types of normal tissue samples, the highest *SEC11A* expression was found in the bone marrow. However, within the nine GC cases, three cases showed *SEC11A* expression levels higher than those in the bone marrow. In the same tissue samples, we also investigated the expression of *SEC11C* (which encodes the SPC21 protein) because of its presumed catalytic activity. In contrast to *SEC11A*, overexpression (GC/normal stomach ratio > 2) of *SEC11C* was detected in 1 (11%) case. Expression of *SEC11A* was analyzed by qRT–PCR in 42 additional GC tissue samples and corresponding non-neoplastic mucosa samples (Figure 1b). Overexpression (GC/corresponding non-neoplastic mucosa ratio > 2) of *SEC11A* was observed in 17 (40%) of the 42 GC cases. Overexpression of *SEC11A* was more frequently found in stage III/IV GC cases (15/24, 63%) than in stage I/II GC cases (2/18, 11%, $P = 0.001$, χ^2-test). These results suggest that, although both *SEC11A* and *SEC11C* encode subunits of SPC, their mRNA expression levels were regulated differently, and only *SEC11A* was overexpressed in GC cases (40%).

Expression and distribution of SPC18 protein in GC tissue

The polyclonal anti-SPC18 antibody generated in our laboratory was detected in a single band of ~18-kDa on western blots of cell extracts from MKN-45 cells (Figure 2a). We confirmed that SPC18 protein was also detected in extracts of the microsomal fraction, which included ER protein (Figure 2a). Furthermore, the 18-kDa band disappeared with preincubation of the antibody with the appropriate SPC18 protein.

We performed immunohistochemical analysis of SPC18 in two independent cohorts: the Hiroshima and Chiba cohorts. First, immunohistochemical analysis was performed in the Hiroshima cohort using whole paraffin-embedded blocks to analyze in detail the expression and distribution of SPC18 protein in GC tissue. In non-neoplastic gastric mucosa, staining of SPC18 was either weak or absent in epithelial and stromal cells, whereas corresponding GC tissue showed relatively stronger, more extensive staining (Figure 2b). SPC18 was detected in the cytoplasm of tumor cells in intestinal-type (Figure 2c) and diffuse-type GC (Figure 2d). The percentage of SPC18-stained tumor cells ranged from 0 to 80%. We confirmed that specific immunostaining was not seen with pre-adsorbed anti-SPC18 antibody (data not shown). When more than 10% of tumor cells were stained, the immunostaining was considered positive for SPC18. In total, 26 (26%) of 99 GC cases were positive for SPC18. SPC18 staining was observed more frequently in stage III/IV cases than in stage I/II cases ($P = 0.002$, χ^2-test, Table 2). We found that SPC18 expression was significantly associated with increased cancer-specific mortality ($P = 0.002$, Log-rank test, Figure 2e). The univariate analysis indicated that expressions of SPC18 (Hazard ratio (HR), 2.71; 95% confidence interval (CI), 1.38–5.37; $P = 0.003$) and tumor stage (HR, 9.62; 95% CI, 3.94–23.26; $P < 0.001$) were associated with survival, while age, sex and histological classification were not. However, in the multivariate model, SPC18 expression was not an independent prognostic indicator (Table 3).

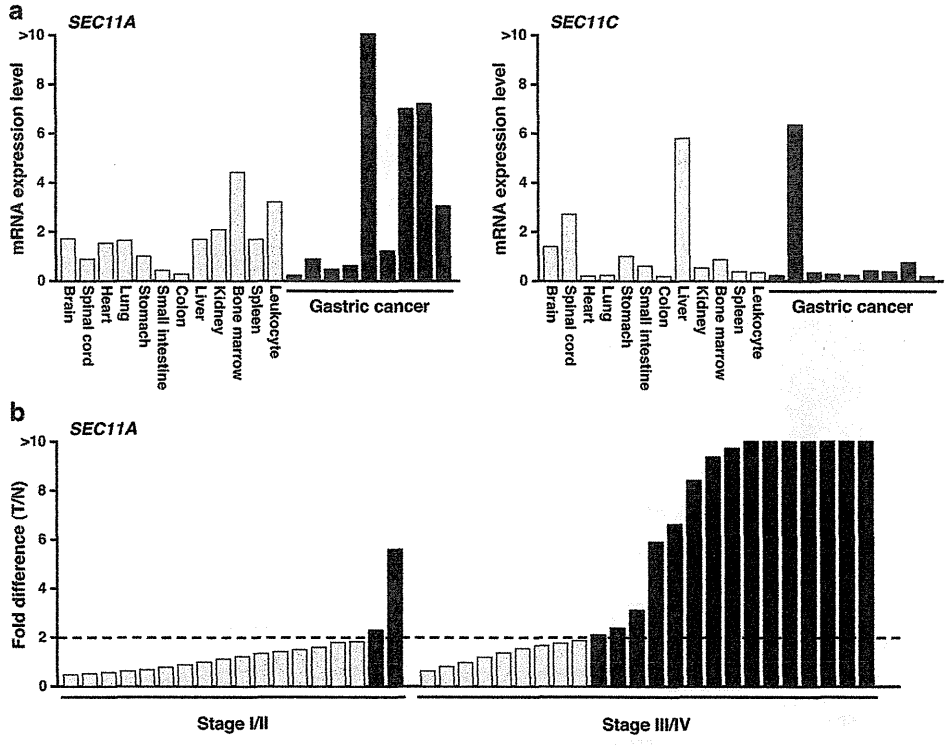

Figure 1. (**a**) qRT–PCR analysis of *SEC11A* and *SEC11C* in 12 normal tissues and nine GC samples. The bars represent individual samples. (**b**) qRT–PCR analysis of SEC11A in 42 GC samples. The bars represent individual samples. Fold change indicates the ratio of SEC11A mRNA level in GC to that in corresponding non-neoplastic mucosa.

Next, immunohistochemical analysis was performed in the Chiba cohort using tissue microarray. When more than 10% of tumor cells were stained, the immunostaining was considered positive for SPC18. In total, 197 (20%) of 989 GC cases were positive for SPC18. SPC18 staining was associated with tumor stage ($P<0.001$, χ^2-test, Table 4). We found that SPC18 expression was significantly associated with increased cancer-specific mortality ($P=0.001$, Log-rank test, Figure 2f). The univariate analysis indicated that expression of SPC18 (HR, 1.73; 95% CI, 1.24–2.39; $P=0.001$) was associated with survival. However, in the multivariate model, SPC18 expression was not an independent prognostic indicator (Table 5).

Forced expression of SPC18 promotes GC cell growth *in vitro* and *in vivo*

The MKN-1 GC cell line was stably transfected with pcDNA-V5-SPC18. MKN-1 cells were selected for low *SEC11A* mRNA expression from among eight different GC cell lines (data not shown). Clones were selected in G418 and examined for SPC18 expression by V5 western blot (Figure 3a). Clones that expressed V5-tagged SPC18 were designated as MKN-1-SPC18-1, MKN-1-SPC18-2 and MKN-1-SPC18-3. Endogenous and exogenous levels of SPC18 protein were also investigated in one western blot with anti-SPC18 antibody to demonstrate the relative overexpression of SPC18. As shown in Figure 3a, MKN-1-SPC18-1, MKN-1-SPC18-2 and MKN-1-SPC18-3 expressed V5-tagged SPC18 protein at significantly higher levels than MKN-1 cells transfected with empty vector. To determine the effect of SPC18 on cell viability *in vitro*, 3-(4,5-Dimethylthiazol-2-yl)-2,5-diphenyltetrazolium bromide (MTT) assays were performed. On day 8, MKN-1 cells transfected with V5-tagged SPC18 showed significantly increased viability compared with MKN-1 cells transfected with pcDNA 3.1 control vector ($P=0.001$, $P=0.001$ and $P=0.001$, respectively, unpaired Student's *t*-test)(Figure 3b). Boyden chamber invasion assays were then performed. V5-tagged SPC18-transfected MKN-1 cells were more invasive than cells transfected with control vector, as measured on day 2 ($P=0.023$ and $P=0.015$, and $P=0.010$. respectively, unpaired Student's *t*-test)(Figure 3c).

We next hypothesized that increased activity of SPC by forced overexpression of SPC18 protein could induce secretion of several types of growth factor associated with cancer cell growth. EGF and TGF-α both phosphorylate the EGF receptor (EGFR) and stimulate multiple signaling pathways involved in cell proliferation, anti-apoptosis and other processes.[16,17] As measured by enzyme-linked immunosorbent assay (ELISA), secretion of TGF-α was high in culture media from the MKN-1 cells stably transfected with pcDNA-V5-SPC18 in comparison with culture media from the MKN-1 cells transfected with pcDNA 3.1 control vector ($P=0.001$, $P=0.001$ and $P=0.001$, respectively, unpaired Student's *t*-test) (Figure 3d). EGF protein, however, was not detected in culture media from MKN-1 cells transfected with pcDNA 3.1 control vector or those transfected with pcDNA-V5-SPC18.

SPC18 and SPC21 are presumed to have catalytic activity to cleave ER signal peptides during protein trafficking from the ER to the extracellular space or to the plasma membrane through the ER–Golgi secretory pathway.[12] This raises a question whether the catalytic activity of SPC18 is required for promoting TGF-α secretion. It has been reported that the high degree of sequence similarity between yeast Sec11p and its canine homologs, SPC18 and SPC21.[12] The alignment shows that canine SPC18 and SPC21 have conserved serine, histidine and aspartic acid residues that are known to be essential for Sec11p catalytic activity. However, catalytic activity of human SPC18 has not been investigated. To examine which part of the SPC18 protein mediates the signal peptidase activity, we generated a NH_2-terminal and COOH-terminal truncation mutant constructs of SPC18 as a fusion protein containing a NH_2-terminal V5 tag

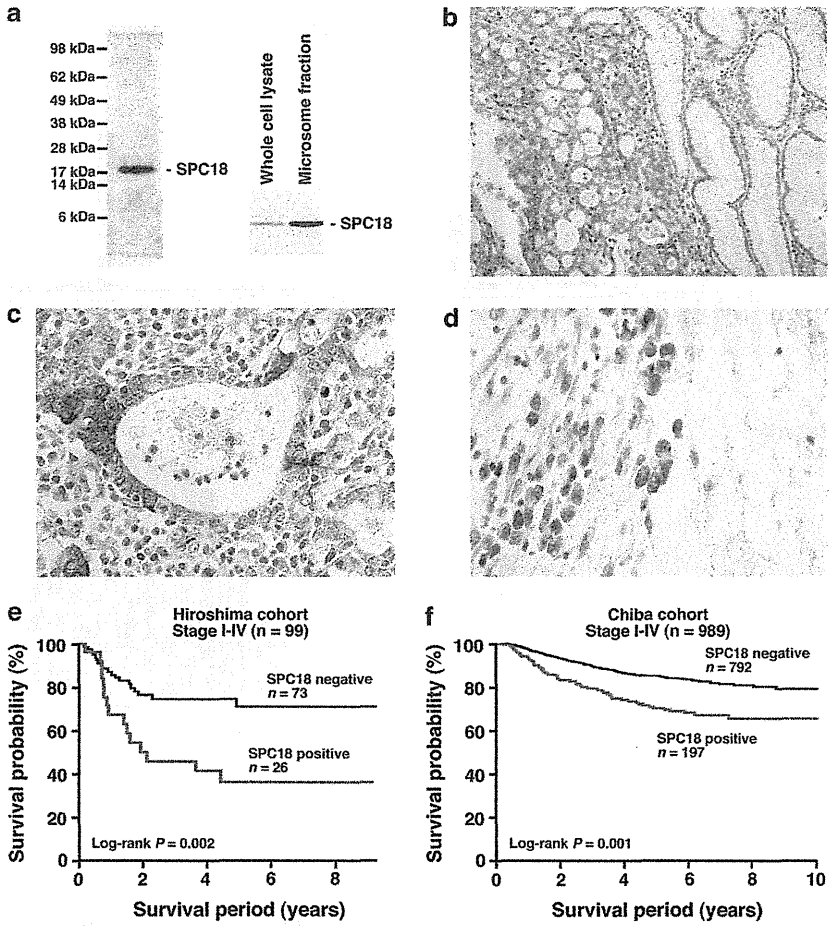

Figure 2. (**a**) Western blot analysis of SPC18 with anti-SPC18 antibody raised in our laboratory. Analysis of MKN-45 cells revealed a band of ~18-kDa. SPC18 protein was also found in the microsomal fraction. (**b**) Immunohistochemical analysis of SPC18 in GC and corresponding non-neoplastic gastric mucosa (original magnification: ×200). (**c**, **d**) Immunohistochemical analysis of SPC18 in (**c**) intestinal-type GC and (**d**) diffuse-type GC (original magnification: ×400). (**e**, **f**) Kaplan–Meier plot of the cancer-specific mortality in the Hiroshima and Chiba cohorts, respectively.

(Figure 3e). To determine if these mutant constructs produce proteins in MKN-1, we transfected MKN-1 cells with each construct and performed western blot analysis using an anti-V5 antibody. Both NH_2-terminal and COOH-terminal truncation mutants produced proteins of the predicted size (Figure 3e). To determine whether these proteins are functional, secretion of TGF-α in culture media was measured by ELISA. The secretion of TGF-α in culture media from the MKN-1 cells transfected with NH_2-terminal or COOH-terminal truncation mutants was similar to that from the MKN-1 cells transfected with pcDNA 3.1 control vector (Figure 3e). These results indicate that SCP18 is involved in maintaining TGF-α secretion in GC cells, and both NH_2-terminal half of the SPC18 protein and COOH-terminal half of the SPC18 protein are required for TGF-α secretion.

It is possible that increased activity of SPC by SPC18 protein upregulation could induce secretion of several types of growth factor associated with cancer cell growth and invasion, and role of TGF-α in invasion remains unclear. Therefore, we asked whether TGF-α is involved in invasion activity in MKN-1 cells. Treatment with TGF-α stimulated the cell invasion activity of MKN-1 cells ($P=0.001$, unpaired Student's *t*-test) (Figure 3c). However, as TGF-α also increased cell viability ($P=0.025$, unpaired Student's *t*-test) (Figure 3b), the cell number difference observed in the invasion assay may be caused by increased cell proliferation activity.

To evaluate the influence of SPC18 on cellular growth *in vivo*, the MKN-1 cells stably transfected with pcDNA-V5-SPC18 were subcutaneously injected into the backs of severe combined immunodeficiency (SCID) mice. As shown in Figure 3f, tumor volume increased much faster in mice injected with MKN-1-SPC18-1 ($n=5$), MKN-1-SPC18-2 ($n=5$) and MKN-1-SPC18-3 ($n=5$) than in mice injected with MKN-1 cells transfected with control vector ($n=5$) ($P=0.001$, $P=0.001$ and $P=0.001$, respectively, unpaired Student's *t*-test). The Ki67 index in tumors injected with MKN-1-SPC18-1 was significantly higher than that in MKN-1 cells transfected with control vector ($P=0.029$, unpaired Student's *t*-test) on day 48 (Figure 3g). The Ki67 index in tumors injected with MKN-1-SPC18-2 and with MKN-1-SPC18-3 was also significantly higher than that in MKN-1 cells transfected with control vector on day 48 ($P=0.029$ and $P=0.029$, respectively, unpaired Student's *t*-test). Because secretion of TGF-α was high in culture media from the MKN-1 cells stably transfected with pcDNA-V5-SPC18 in comparison with culture media from the MKN-1 cells transfected with pcDNA 3.1 control vector, phosphorylation of EGFR in mouse tumors on day 48 was examined by western blot (Figure 3h). Phosphorylation of EGFR at Tyr1068 in tumors injected with MKN-1-SPC18-1, MKN-1-SPC18-2 and MKN-1-SPC18-3 was significantly higher than that in tumors injected with MKN-1 cells transfected with control vector. We also examined the activation of downstream effector of the EGFR pathway. Phosphorylation of

Table 2. Relationship between SPC18 expression and clinicopathologic characteristics in the Hiroshima cohort

	SPC18 expression		P-*value*[a]
	Positive	*Negative*	
Age			
<66	7 (22%)	25	0.658
⩾66	19 (28%)	48	
Sex			
Male	10 (22%)	35	0.545
Female	16 (30%)	38	
T classification			
T1/2	5 (16%)	27	0.142
T3/4	21 (31%)	46	
N classification			
N0	9 (21%)	33	0.368
N1/2/3	17 (30%)	40	
Tumor stage			
Stage I/II	8 (14%)	48	0.002
Stage III/IV	18 (42%)	25	
Histological classification			
Intestinal	16 (30%)	37	0.369
Diffuse	10 (7%)	36	

[a]χ^2-test.

Table 3. Univariate and multivariate Cox regression analysis of SPC18 expression and survival in the Hiroshima cohort

Characteristic	*Univariate analysis*		*Multivariate analysis*	
	HR (95% CI)	P-*value*	*HR (95% CI)*	P-*value*
SPC18 expression				
Negative	1 (Ref.)		1 (Ref.)	
Positive	2.71 (1.38–5.37)	0.003	1.56 (0.78–3.13)	0.206
Tumor stage				
I/II	1 (Ref.)		1 (Ref.)	
III/IV	9.62 (3.94–23.26)	<0.001	8.55 (2.13–21.28)	<0.001
Age				
66 and >66	1 (Ref.)			
<66	1.21 (0.62–2.38)	0.573		
Sex				
Female	1 (Ref.)			
Male	1.06 (0.54–2.11)	0.856		
Histologic classification				
Intestinal	1 (Ref.)			
Diffuse	1.52 (0.77–2.99)	0.227		

Abbreviations: HR, hazard ratio; CI, confidence interval.

Table 4. Relationship between SPC18 expression and clinicopathologic characteristics in the Chiba cohort

	SPC18 expression		P *value*[a]
	Positive	*Negative*	
Age			
<66	104 (19%)	454	0.245
⩾66	93 (22%)	338	
Sex			
Male	150 (23%)	515	0.736
Female	47 (15%)	277	
T classification			
T1	52 (11%)	438	<0.001
T2	22 (18%)	103	
T3	76 (34%)	150	
T4	47 (32%)	101	
N classification			
N0	79 (13%)	519	<0.001
N1/2/3	118 (30%)	273	
Tumor stage			
Stage I	54 (10%)	475	<0.001
Stage II	68 (32%)	143	
Stage III	50 (29%)	125	
Stage IV	25 (34%)	49	
Histological classification			
Intestinal	124 (26%)	358	<0.001
Diffuse	73 (14%)	434	

[a]χ^2 test.

Table 5. Univariate and multivariate Cox regression analysis of SPC18 expression and survival in the Chiba cohort

Characteristic	*Univariate analysis*		*Multivariate analysis*	
	HR (95% CI)	P *value*	*HR (95% CI)*	P-*value*
SPC18 expression				
Negative	1 (Ref.)		1 (Ref.)	0.807
Positive	1.73 (1.24–2.39)	0.001	1.04 (0.74–1.45)	
Tumor stage				
I	1 (Ref.)		1 (Ref.)	
II	4.06 (2.47–6.65)	<0.001	4.06 (2.43–6.77)	<0.001
III	11.01 (7.02–17.27)	<0.001	10.43 (6.50–16.72)	<0.001
IV	37.39 (22.65–61.729)	<0.001	38.70 (22.83–65.60)	<0.001
Age				
⩾66				
<66				
Sex				
Female	1 (Ref.)		1 (Ref.)	
Male	1.48 (1.06–2.07)	0.021	1.57 (1.34–1.57)	0.012
Histologic classification				
Intestinal	1 (Ref.)	0.009	1 (Ref.)	0.014
Diffuse	1.49 (1.10–2.01)		1.48 (1.08–2.04)	

Abbreviations: HR, hazard ratio; CI, confidence interval.

AKT, which is one of the downstream effectors of EGFR pathway,[18] was examined by western blot (Figure 3h). Phosphorylation of AKT at Ser473 in tumors injected with MKN-1-SPC18-1, MKN-1-SPC18-2 and MKN-1-SPC18-3 was significantly higher than that in tumors injected with MKN-1 cells transfected with control vector. These results indicate that forced expression of SPC18 can promote tumor growth *in vitro* and *in vivo*.

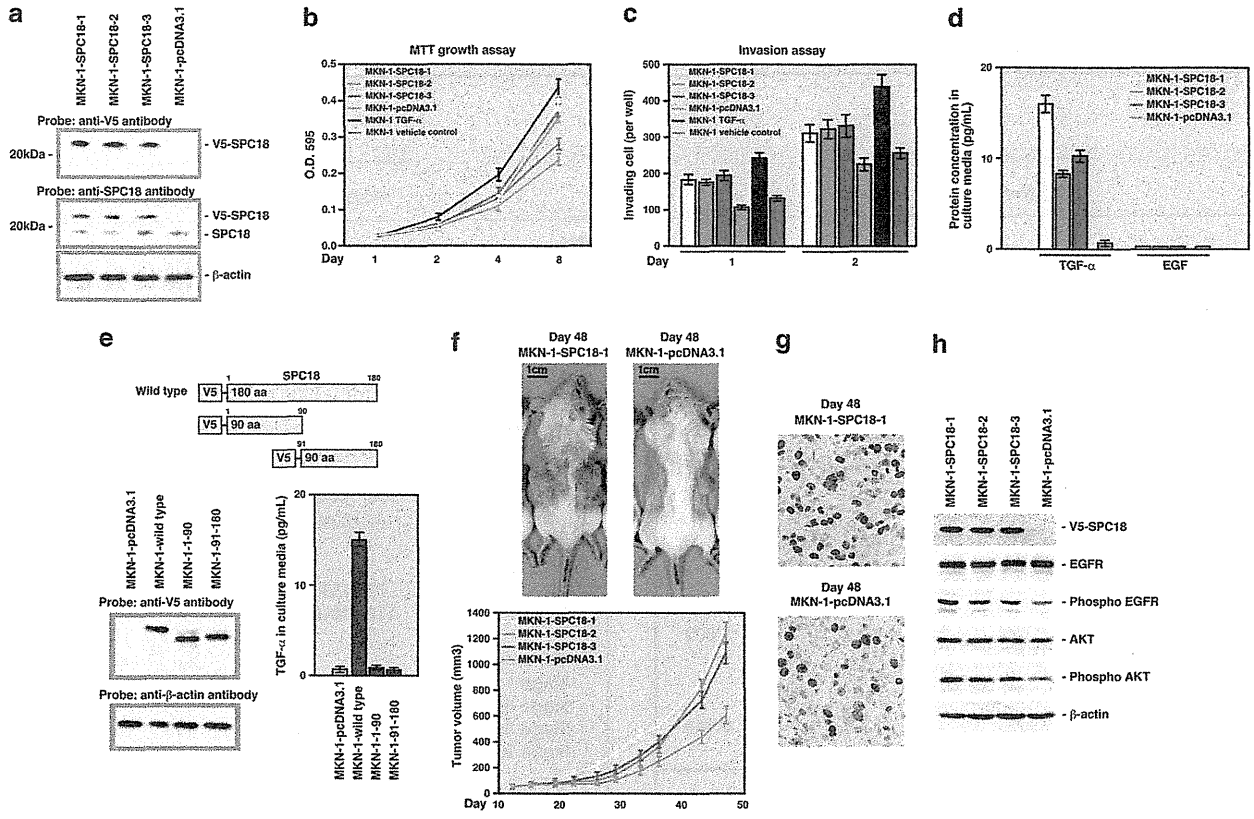

Figure 3. (**a**) Western blot analysis of V5-tagged SPC18 with an anti-V5 antibody or anti-SPC18 antibody in the MKN-1 cell line stably transfected with pcDNA-V5-SPC18 or pcDNA 3.1. (**b**) Effect of V5-tagged SPC18 or TGF-α treatment on MKN-1 cell viability. Cell viability was assessed by MTT assay at days 1, 2, 4 and 8 after seeding on 96-well plates. Bars and error bars indicate mean and s.d., respectively, of three different experiments. (**c**) Effect of V5-tagged SPC18 or TGF-α treatment on cell invasion. MKN-1 cells transfected with pcDNA-V5-SPC18 or pcDNA 3.1 or MKN-1 cells treated with TGF-α were incubated in Boyden chambers. After 1 and 2 days, invading cells were counted. Bars and error bars indicate mean and s.d., respectively, of three different experiments. (**d**) TGF-α and EGF protein levels in culture media of MKN-1 cells transfected with pcDNA-V5-SPC18 or pcDNA 3.1 were measured by ELISA. Bars and error bars indicate mean and s.d., respectively, of three different experiments. (**e**) A schematic diagram of SPC18 truncation mutants. V5 indicates NH2-terminal V5 tag. Amino-acid residues are shown on the top of each construct. Expression of each mutant was confirmed in MKN-1 cells transfected with each construct by western blot analysis using anti-V5 antibody. TGF-α protein levels in culture media of MKN-1 cells transfected with each construct were measured by ELISA. Bars and error bars indicate mean and s.d., respectively, of three different experiments. (**f**) The MKN-1 cells stably transfected with pcDNA-V5-SPC18 or pcDNA 3.1 were injected into SCID mice. Bars and error bars indicate mean and s.d., respectively, of five mice. (**g**) Immunohistochemical analysis of Ki67 in mouse tumor transfected with pcDNA-V5-SPC18 or pcDNA 3.1 (original magnification: ×400). (**h**) Western blot analysis of V5-taggd SPC18, EGFR, phospho-EGFR (Tyr1068), AKT and phospho-AKT (Ser473) in mouse tumor transfected with pcDNA-V5-SPC18 or pcDNA 3.1.

SPC18 is associated with TGF-α secretion

We analyzed by ELISA the effect of inhibiting SPC18 expression by RNAi on the secretion of TGF-α and EGF by MKN-45 cells because high endogenous SPC18 expression was detected in MKN-45 cells. The expression of SPC18 in MKN-45 cells was suppressed by treatment with siRNA1 and siRNA2 2 days after transfection (Figure 4a), and the levels of TGF-α in culture media from the MKN-45 cells transfected with SPC18 siRNA1 or SPC18 siRNA2 were significantly lower than those from MKN-45 cells transfected with negative control siRNA ($P=0.001$ and $P=0.001$, respectively, unpaired Student's *t*-test) (Figure 4b). We measured mRNA expression levels of TGF-α by qRT–PCR, however, mRNA expression levels of TGF-α in the MKN-45 cells transfected with SPC18 siRNA1 or SPC18 siRNA2 were similar to those in the MKN-45 cells transfected with negative control siRNA. EGF protein was not detected in culture media from the MKN-45 cells transfected with SPC18 siRNA or those transfected with negative control siRNA by ELISA.

Microsome fraction, which included ER protein, was extracted, and the levels of TGF-α were measured by ELISA. As shown in Figure 4b, the levels of TGF-α in microsome fraction from the MKN-45 cells transfected with SPC18 siRNA1 or SPC18 siRNA2 were significantly higher than those from MKN-45 cells transfected with negative control siRNA ($P=0.001$ and $P=0.001$, respectively, unpaired Student's *t*-test). These results indicate that SCP18 is involved in maintaining TGF-α secretion in GC cells.

To investigate the possible antiproliferative effects of SPC18 knockdown, we performed an MTT assay 8 days after siRNA transfection (Figure 4c). MKN-45 siRNA1-transfected and siRNA2-transfected MKN-45 cells showed significantly reduced viability relative to negative control siRNA-transfected MKN-45 cells ($P=0.001$ and $P=0.001$, respectively, unpaired Student's *t*-test). Next, to determine the possible role of SPC18 in the invasiveness of GC cells, we used a transwell invasion assay (Figure 4d). On day 2, the invasiveness of SPC18-knockdown MKN-45 cells was ~50% less than that of the negative control siRNA-transfected MKN-45 cells ($P=0.007$ and $P=0.005$, respectively, unpaired Student's *t*-test). However, as SPC18-knockdown cells showed significantly reduced cell viability, the cell number difference observed in the invasion assay may be caused by the reduced cell viability.

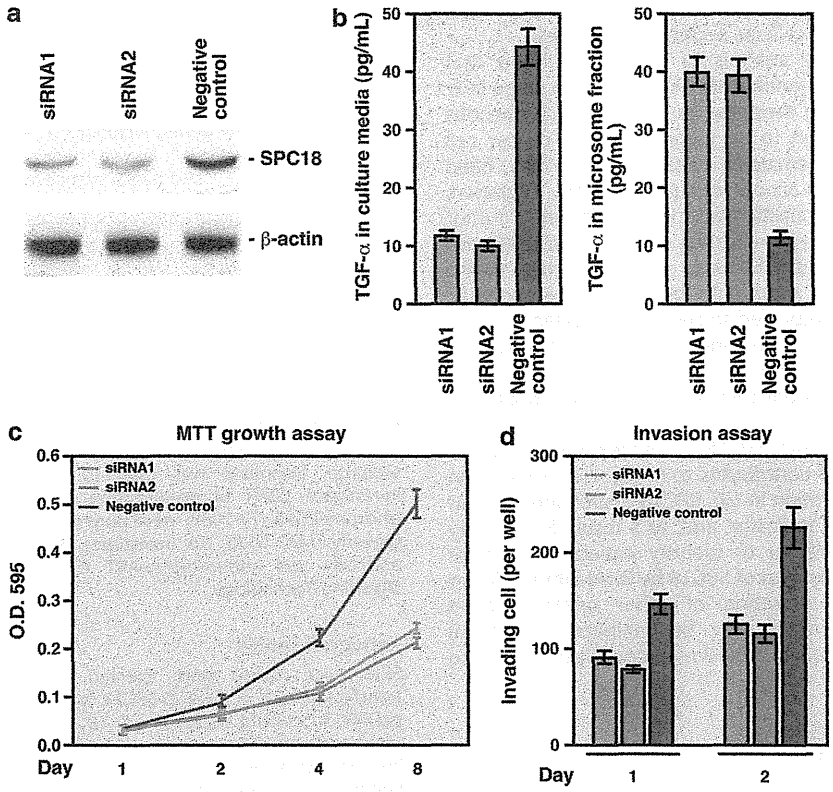

Figure 4. (**a**) Western blot analysis of SPC18 in MKN-45 cells transfected with the SPC18 siRNA (siRNA1 and 2) and negative control siRNA. (**b**) TGF-α protein levels in the culture media or microsome fraction of MKN-45 cells transfected with SPC18 siRNA (siRNA1 and 2) and negative control siRNA. Bars and error bars indicate mean and s.d., respectively, of the three different experiments. (**c**) Effect of SPC18 knockdown on MKN-45 cell viability. Cell viability was assessed using MTT assay at days 1, 2, 4 and 8 after seeding on 96-well plates. Bars and error bars indicate mean and s.d., respectively, of three different experiments. (**d**) Effect of SPC18 knockdown on cell invasion in MKN-45 cells. MKN-45 cells transfected with SPC18 siRNA (siRNA1 and 2) or negative control siRNA were incubated in Boyden chambers. After 1 and 2 days, invading cells were counted. Bars and error bars indicate mean and s.d., respectively, of three different experiments.

Taken together, these results indicate that SPC18 contributes to cancer cell progression via TGF-α secretion.

DISCUSSION

In the present study, we built a small and focused oligonucleotide array on which 394 genes were selected based on our SAGE data and previously reported array data, and found that *SEC11A*, which encodes SPC18 protein, is overexpressed in GC. Although growth factors such as TGF-α and EGF have an important role in cancer cell growth, the possible effects of alteration to cellular secretion mechanisms on the secretion of these oncogenic factors have not been investigated. We showed that expression levels of SPC18 varied in association with tumor stage in both the Hiroshima and Chiba cohorts. Forced expression of SPC18 in the GC cell line promoted cancer cell growth *in vitro* and *in vivo*, and stimulated cancer cell invasion. Furthermore, forced expression of SPC18 induced TGF-α secretion. Knockdown of SPC18 by RNAi inhibited TGF-α secretion. Taken together, these results indicate that SPC18 is associated with GC cell progression rather than GC pathogenesis.

TGF-α is biosynthesized as a larger transmembrane protein termed pro-TGF-α (TGF-α precursor).[19,20] TGF-α precursor contains an extracellular domain of ~100 amino acids that includes the NH_2-terminal signal sequence and the 50-amino acid TGF-α, a hydrophobic transmembrane domain, and a 35-residue cytoplasmic domain.[21] The NH_2-terminal signal sequence allows translocation of the nascent polypeptide chain through the membrane of the ER.[19,20] Three proteolytic events contribute to the complete maturation of the TGF-α precursor. The first event involves the removal of the signal peptide by signal peptidases. This occurs upon the precursor peptide's entry into the secretory route in the ER. In the present study, SPC18 inhibition by RNAi did not change mRNA expression levels of TGF-α in the MKN-45 cells, although SPC18 inhibition reduced TGF-α protein levels in culture media, suggesting that SPC18 overexpression does not upregulate TGF-α expression at the transcriptional level. We also confirmed that the levels of TGF-α in microsome fraction from the NKN-45 cells transfected with SPC18 siRNA1 or SPC18 siRNA2 were significantly higher than those from MKN-45 cells transfected with negative control siRNA. It is likely that SPC18 cleaves the signal peptide of TGF-α within the ER, and that the overexpression of SPC18 enhances secretion of TGF-α.

SPC reportedly has five distinct subunits[11] of which both SPC18 and SPC21 are presumed to have catalytic activity.[12] Although overexpression of SPC18 has frequently been found in GC tissue samples, overexpression of SPC21 was not detected in this study. These results led us to question whether overexpression of SPC18 alone is sufficient to induce high signal peptidase activity in SPC. We confirmed that the knockdown of SPC21 by RNAi inhibits TGF-α secretion in MKN-45 cells (data not shown), indicating that SPC21 is required for maximal signal peptidase activity of the SPC. In contrast, TGF-α secretion can be induced in MKN-1 GC cells by forced expression of SPC18, without SPC21 overexpression (data not shown), suggesting a requirement for further investigation to elucidate possible additional functions of SPC18, as well as

interactions between SPC18 with other subunits of the SPC and other molecules involved in cellular secretion processes.

The oligonucleotide array analysis in this study found that expression of six genes was significantly higher in GC at stage III/IV than GC at stage I/II. Among these genes, *MMP7*, which encodes matrilysin, has been reported to be associated with cancer cell invasion.[14] *TDGF1*, which encodes cripto protein, has been reported to be involved in cancer cell proliferation, migration, epithelial-to-mesenchymal transition and in stimulation of tumor angiogenesis.[22] However, the significance of *DDOST*, *NDUFB7* and *SUPT4H1* remains unclear. *DDOST* has been reported to be associated with cancer cell metastasis by microarray analysis.[6] *NDUFB7*and *SUPT4H1* were reported to be overexpressed in GC in our SAGE analysis.[2] To further our understanding of the role of these genes in GC, detailed expression analysis using methods such as qRT–PCR or immunohistochemical analysis should be performed.

In summary, we found that SPC18 is overexpressed in GC. We also showed that SPC18 contributes to malignant progression by promotion of TGF-α secretion in GC. SPC18 expression was not an independent prognostic indicator, and, as a result, SPC18 may not be suitable as a biomarker to identify patients with poor prognosis. In contrast, knockdown of SPC18 by RNAi inhibits TGF-α secretion, indicating that secretion of other growth factors promoting cancer cell growth may be inhibited by SPC18 knockdown. Specific inhibitors of SPC18 may constitute promising anticancer drugs.

MATERIALS AND METHODS

Tissue samples

In all, 1164 primary tumors were collected from patients diagnosed with GC. The samples were obtained during surgery at the Hiroshima University Hospital or an affiliated hospital. We confirmed microscopically that the tumor specimens were predominantly (>80%) cancer tissue. Samples were frozen immediately in liquid nitrogen and stored at −80 °C until use. Twenty-five GC samples and corresponding non-neoplastic mucosal samples were obtained for use in our oligonucleotide array analysis.

For qRT–PCR analysis, the noncancerous samples of heart, lung, stomach, small intestine, colon, liver, pancreas, kidney, bone marrow, peripheral leukocytes, spleen, skeletal muscle, brain and spinal cord were purchased from Clontech (Palo Alto, CA, USA). In total, fifty-one GC samples and corresponding non-neoplastic mucosa samples were used for qRT–PCR analysis.

For immunohistochemical analysis, we used archival formalin-fixed, paraffin-embedded tissues from 1088 patients who had undergone surgical excision of GC. Of these patients, 99 had been treated at the Hiroshima University Hospital, Hiroshima, Japan (Hiroshima cohort); the remaining 989 were treated at the National Cancer Center Hospital East, Chiba, Japan (Chiba cohort). Immunohistochemical analysis was performed using whole paraffin-embedded blocks for the Hiroshima cohort and tissue microarray for the Chiba cohort.[23] This study was approved by the Ethical Committee for Human Genome Research of Hiroshima University and the institutional review board of the National Cancer Center.

Cell lines, expression vector, transfection and TGF-α treatment

MKN-1 and MKN-45 GC cell lines were provided by Dr Toshimitsu Suzuki.[24] All cell lines were maintained in RPMI 1640 (Nissui Pharmaceutical Co., Ltd., Tokyo, Japan) containing 10% fetal bovine serum (BioWhittaker, Walkersville, MD, USA) in a humidified atmosphere of 5% CO_2 and 95% air at 37 °C. For constitutive expression of the *SEC11A* gene, cDNA was PCR amplified and subcloned into pcDNA 3.1 (Invitrogen Corp., Carlsbad, CA, USA) in-frame with a NH_2-terminal (pcDNA-V5-SPC18) V5 epitope tag. Transient transfection was carried out with FuGENE6 Transfection Reagent (Roche Diagnostics, Indianapolis, IN, USA). After 24 h of serum starvation, 100 nM concentration of TGF-α (Sigma, St Louis, MO, USA) was added.

Oligonucleotide array construction and data analysis

The 70-nucleotide oligonucleotides were synthesized with amino-modified 5′ termini (Oligator Human Refset, Illumina, San Diego, CA, USA). The oligonucleotides were dissolved in 40 μl of Solution I (Takara Bio Inc., Shiga, Japan), and then spotted in triplicate onto glass slides (Hubble Slide, Takara Bio Inc.) using a GMS 417 Arrayer (Affymetrix, Santa Clara, CA, USA). Slides were fixed in 0.2% SDS for 2 min and in 0.3 N NaOH for 5 min, then dehydrated with 100% cold ethanol for 3 min and finally air-dried. The array contained 394 genes, including GC-related genes identified by our previous SAGE analysis,[2] known genes related to development and progression of GC,[6–8] and genes associated with sensitivity to anticancer drugs.[9] A list of the genes on the array is available upon request. Preparation of labeled probe, hybridization, detection and data analysis were performed as described previously.[25]

Antibodies

Rabbit polyclonal antibodies were raised against His-tagged recombinant SPC18 produced in bacteria and purified with nickel resin (Qiagen, Valencia, CA, USA). Specificity of the anti-SPC18 antibody was evaluated by ELISA. Immunoreactive sera were affinity-purified with the His-tagged recombinant SPC18 protein. An anti-V5 monoclonal antibody was purchased from Invitrogen. An anti-Ki67 antibody (Dako Cytomation, Glostrup, Denmark) was used to measure proliferative activity. To investigate EGFR phosphorylation, an anti-EGFR antibody and anti-phospho-EGFR (Tyr1068) were purchased from Cell Signaling Technology (Beverly, MA, USA). To investigate AKT phosphorylation, an anti-AKT antibody and anti-phospho-AKT (Ser473) were purchased from Cell Signaling Technology.

Xenograft model

SCID mice (CLEA) were injected subcutaneously with MKN-1 cells transfected with pcDNA-V5-SPC18 ($n=5$) or MKN-1 cells transfected with pcDNA 3.1 control vector ($n=5$; 10^7 cells in 0.1 ml of PBS). Tumors were measured with calipers on days 12, 15, 19, 22, 26, 29, 33, 37, 42 and 48 post injection, by which time they had become palpable and visible. Tumor volumes were calculated using the equation: $\text{width}^2 \times \text{length} \times 0.5$. Subcutaneous tumors were surgically excised, weighed and photographed, and a portion of each tumor was placed in 10% formalin for paraffin embedding and subsequent immunohistochemical analysis. Animal protocols were approved by the committee for Ethics of Animal Experimentation and were in accordance with the Guidelines for Animal Experiments in the National Cancer Center.

The following were used in this study: qRT–PCR analysis, western blot analysis, immunohistochemical analysis, cell viability and *in vitro* invasion assays, RNAi, measurement of TGF-α and EGF, and statistical methods.

Detailed information is described in the Supplementary Data.

CONFLICT OF INTEREST

The authors declare no conflict of interest.

ACKNOWLEDGEMENTS

We thank Mr Shinichi Norimura for excellent technical assistance and advice. This work was carried out with the kind cooperation of the Research Center for Molecular Medicine, Faculty of Medicine, Hiroshima University. We thank the Analysis Center of Life Science, Hiroshima University, for the use of their facilities.

REFERENCES

1 Yasui W, Sentani K, Sakamoto N, Anami K, Naito Y, Oue N. Molecular pathology of gastric cancer: research and practice. *Pathol Res Pract* 2011; **207**: 608–612.
2 Oue N, Hamai Y, Mitani Y, Matsumura S, Oshimo Y, Aung PP *et al.* Gene expression profile of gastric carcinoma: identification of genes and tags potentially involved in invasion, metastasis, and carcinogenesis by serial analysis of gene expression. *Cancer Res* 2004; **64**: 2397–2405.
3 Aung PP, Oue N, Mitani Y, Nakayama H, Yoshida K, Noguchi T *et al.* Systematic search for gastric cancer-specific genes based on SAGE data: melanoma inhibitory activity and matrix metalloproteinase-10 are novel prognostic factors in patients with gastric cancer. *Oncogene* 2006; **25**: 2546–2557.
4 Mitani Y, Oue N, Matsumura S, Yoshida K, Noguchi T, Ito M *et al.* Reg IV is a serum biomarker for gastric cancer patients and predicts response to 5-fluorouracil-based chemotherapy. *Oncogene* 2007; **26**: 4383–4393.
5 Oue N, Sentani K, Noguchi T, Ohara S, Sakamoto N, Hayashi T *et al.* Serum olfactomedin 4 (GW112, hGC-1) in combination with Reg IV is a highly sensitive biomarker for gastric cancer patients. *Int J Cancer* 2009; **125**: 2383–2392.

6 Hippo Y, Yashiro M, Ishii M, Taniguchi H, Tsutsumi S, Hirakawa K *et al.* Differential gene expression profiles of scirrhous gastric cancer cells with high metastatic potential to peritoneum or lymph nodes. *Cancer Res* 2001; **61**: 889–895.
7 Hippo Y, Taniguchi H, Tsutsumi S, Machida N, Chong JM, Fukayama M *et al.* Global gene expression analysis of gastric cancer by oligonucleotide microarrays. *Cancer Res* 2002; **62**: 233–240.
8 Hasegawa S, Furukawa Y, Li M, Satoh S, Kato T, Watanabe T *et al.* Genome-wide analysis of gene expression in intestinal-type gastric cancers using a complementary DNA microarray representing 23 040 genes. *Cancer Res* 2002; **62**: 7012–7017.
9 Zembutsu H, Ohnishi Y, Tsunoda T, Furukawa Y, Katagiri T, Ueyama Y *et al.* Genome-wide cDNA microarray screening to correlate gene expression profiles with sensitivity of 85 human cancer xenografts to anticancer drugs. *Cancer Res* 2002; **62**: 518–527.
10 Nickel W, Rabouille C. Mechanisms of regulated unconventional protein secretion. *Nat Rev Mol Cell Biol* 2009; **10**: 148–155.
11 Greenburg G, Shelness GS, Blobel G. A subunit of mammalian signal peptidase is homologous to yeast SEC11 protein. *J Biol Chem* 1989; **264**: 15762–15765.
12 Shelness GS, Blobel G. Two subunits of the canine signal peptidase complex are homologous to yeast SEC11 protein. *J Biol Chem* 1990; **265**: 9512–9519.
13 Ueda M, Fujii H, Yoshizawa K, Terai Y, Kumagai K, Ueki K *et al.* Effects of EGF and TGF-alpha on invasion and proteinase expression of uterine cervical adenocarcinoma OMC-4 cells. *Invasion Metastasis* 1998–1999; **18**: 176–183.
14 Ii M, Yamamoto H, Adachi Y, Maruyama Y, Shinomura Y. Role of matrix metalloproteinase-7 (matrilysin) in human cancer invasion, apoptosis, growth, and angiogenesis. *Exp Biol Med (Maywood)* 2006; **231**: 20–27.
15 Yasui W, Tahara E, Tahara H, Fujimoto J, Naka K, Nakayama J *et al.* Immunohistochemical detection of human telomerase reverse transcriptase in normal mucosa and precancerous lesions of the stomach. *Jpn J Cancer Res* 1999; **90**: 589–595.
16 Kang MJ, Ryu BK, Lee MG, Han J, Lee JH, Ha TK *et al.* NF-kappaB activates transcription of the RNA-binding factor HuR, via PI3K-AKT signaling, to promote gastric tumorigenesis. *Gastroenterology* 2008; **135**: 2030–2042.
17 Regalo G, Resende C, Wen X, Gomes B, Duraes C, Seruca R *et al.* C/EBP alpha expression is associated with homeostasis of the gastric epithelium and with gastric carcinogenesis. *Lab Invest* 2010; **90**: 1132–1139.
18 Dedes KJ, Wetterskog D, Ashworth A, Kaye SB, Reis-Filho JS. Emerging therapeutic targets in endometrial cancer. *Nat Rev Clin Oncol* 2011; **8**: 261–271.
19 Teixidó J, Gilmore R, Lee DC, Massagué J. Integral membrane glycoprotein properties of the prohormone pro-transforming growth factor-alpha. *Nature* 1987; **326**: 883–885.
20 Bringman TS, Lindquist PB, Derynck R. Different transforming growth factor-alpha species are derived from a glycosylated and palmitoylated transmembrane precursor. *Cell* 1987; **48**: 429–440.
21 Lee DC, Rose TM, Webb NR, Todaro GJ. Cloning and sequence analysis of a cDNA for rat transforming growth factor-alpha. *Nature* 1985; **313**: 489–491.
22 de Castro NP, Rangel MC, Nagaoka T, Salomon DS, Bianco C. Cripto-1: an embryonic gene that promotes tumorigenesis. *Future Oncol* 2010; **6**: 1127–1142.
23 Nitadori J, Ishii G, Tsuta K, Yokose T, Murata Y, Kodama T *et al.* Immunohistochemical differential diagnosis between large cell neuroendocrine carcinoma and small cell carcinoma by tissue microarray analysis with a large antibody panel. *Am J Clin Pathol* 2006; **125**: 682–692.
24 Motoyama T, Hojo H, Watanabe H. Comparison of seven cell lines derived from human gastric carcinomas. *Acta Pathol Jpn* 1986; **36**: 65–83.
25 Inoue H, Matsuyama A, Mimori K, Ueo H, Mori M. Prognostic score of gastric cancer determined by cDNA microarray. *Clin Cancer Res* 2002; **8**: 3475–3479.

Supplementary Information accompanies this paper on the Oncogene website (http://www.nature.com/onc)

IJC
International Journal of Cancer

High miR-21 expression from FFPE tissues is associated with poor survival and response to adjuvant chemotherapy in colon cancer

Naohide Oue[1,2], Katsuhiro Anami[1,2], Aaron J. Schetter[1], Markus Moehler[3], Hirokazu Okayama[1], Mohammed A. Khan[1], Elise D. Bowman[1], Annett Mueller[3], Arno Schad[3], Manabu Shimomura[4], Takao Hinoi[4], Kazuhiko Aoyagi[5], Hiroki Sasaki[5], Masazumi Okajima[6], Hideki Ohdan[4], Peter R. Galle[3], Wataru Yasui[2] and Curtis C. Harris[1]

[1] Laboratory of Human Carcinogenesis, Center for Cancer Research, National Cancer Institute, National Institutes of Health, Bethesda, MD
[2] Department of Molecular Pathology, Hiroshima University Graduate School of Biomedical Sciences, Hiroshima, Japan
[3] First Department of Internal Medicine, Johannes Gutenberg University of Mainz, Mainz, Germany
[4] Department of Surgery, Hiroshima University Hospital, Hiroshima, Japan
[5] Division of Integrative Omics and Bioinformatics, Innovative Pathophysiology Research Group, National Cancer Center Research Institute, Tokyo, Japan
[6] Department of Endoscopic Surgery and Surgical Science, Hiroshima University, Hiroshima, Japan

Colon cancer (CC) is a leading cause of cancer mortality. Novel biomarkers are needed to identify CC patients at high risk of recurrence and those who may benefit from therapeutic intervention. The aim of this study is to investigate if miR-21 expression from RNA isolated from formalin-fixed paraffin-embedded (FFPE) tissue sections is associated with prognosis and therapeutic outcome for patients with CC. The expression of miR-21 was measured by quantitative reverse transcriptase-polymerase chain reaction in a Japanese cohort (stage I-IV, $n = 156$) and a German cohort (stage II, $n = 145$). High miR-21 expression in tumors was associated with poor survival in both the stage II/III Japanese ($p = 0.0008$) and stage II German ($p = 0.047$) cohorts. These associations were independent of other clinical covariates in multivariable models. Receipt of adjuvant chemotherapy was not beneficial in patients with high miR-21 in either cohort. In the Japanese cohort, high miR-21 expression was significantly associated with poor therapeutic outcome ($p = 0.0001$) and adjuvant therapy was associated with improved survival in patients with low miR-21 ($p = 0.001$). These results suggest that miR-21 is a promising biomarker to identify patients with poor prognosis and can be accurately measured in FFPE tissues. The expression of miR-21 may also identify patients who will benefit from adjuvant chemotherapy.

Epidemiology

Colorectal cancer is a leading cause of cancer mortality worldwide. Adjuvant chemotherapy after surgical resection decreases recurrences and improves survival in stage III colon cancer (CC).[1] Yet current adjuvant therapy does not work equally well for all patients and identifying classifiers to predict response to therapies will help guide medical decisions and result in improved patient outcomes. The role of adjuvant chemotherapy for stage II CC remains controversial. Many stage II patients will benefit from therapy. But if surgery is curative, additional therapy may harm quality of life with little therapeutic benefit. The high-risk features of stage II CC patients include T4 tumors, poor differentiation, perforation, and an inadequate number of evaluated lymph nodes.[2] Yet these features cannot completely identify which patients are at low- or high-risk for disease recurrence. Therefore, it is important to develop novel biomarkers to identify high-risk patients who may be suitable for therapeutic intervention.

Cancer develops as a result of multiple genetic and epigenetic alterations.[3] Better knowledge about the changes in gene expression that occur during carcinogenesis may lead to improvements in diagnosis, treatment, and prevention. Identifying novel biomarkers that can guide therapeutic decisions is a major goal. Although several RNA-based biomarkers have been reported to identify high-risk patients,[4–6] measurement methods of these biomarkers usually require freshly frozen tissues. In contrast, formalin-fixed paraffin-embedded (FFPE) tissue samples have been collected through decades of

Key words: microRNA, prognosis, colorectal cancer
Additional Supporting Information may be found in the online version of this article.
Grant sponsor: Intramural Research Program of the National Cancer Institute, National Institutes of Health, a Department of Defense Congressionally Directed Medical Research Program; **Grant number:** PR093793; **Grant sponsor:** Ministry of Health, Labour and Welfare for the 3rd-term Comprehensive 10-year Strategy for Cancer Control, Japan; **Grant number:** FKN 01KN1103
DOI: 10.1002/ijc.28522
History: Received 8 May 2013; Accepted 27 Aug 2013; Online 5 Oct 2013
Correspondence to: Curtis C. Harris, Laboratory of Human Carcinogenesis, National Cancer Institute, National Institutes of Health, 37 Convent Drive, Building 37, Room 3068, Bethesda, MD 20892, USA, Tel.: 301-496-2048, Fax: 301-496-0497, E-mail: curtis_harris@nih.gov

What's new?

While many stage II colorectal cancer patients benefit from adjuvant therapy, others may be harmed, making the decision to use additional chemotherapy in these populations controversial. This study describes a candidate biomarker, miR-21, that could help overcome this problem. High expression of miR-21 in formalin-fixed paraffin-embedded (FFPE) tissues was associated with poor survival in two independent cohorts of colon cancer patients from Japan and Germany. Low miR-21 expression, on the other hand, was associated with improved survival with adjuvant therapy.

routine histopathological examination and are the most widely available materials for use in clinical research. For evaluation of biomarkers in FFPE tissue, immunohistochemistry or *in situ* hybridization is currently the diagnostic standard. However, the degree of expression of the marker can only be described in a semiquantitative way. In contrast, quantitative reverse transcriptase-polymerase chain reaction (qRT-PCR) is a quantitative, reliable, and standardized method to investigate RNA expression. But formaldehyde-containing fixatives cause cross-linkage between nucleic acids and proteins and make subsequent extraction and quantification of RNA challenging.[7] A major obstacle to RNA expression analysis of FFPE tissues has been the uncertainty about whether gene expression analyses from routinely archived tissues accurately reflect the expression before fixation, and this is likely due to high fragmentation.[8] Because fragmentation does not cause further loss of quality when naturally occurring small RNAs are targeted, microRNA is more ideal for analysis of RNA extracted from FFPE samples.

MicroRNAs are ^{18}- to ^{25}-nucleotide, noncoding RNA molecules that regulate the translation of many genes.[9] MicroRNA expression levels are altered in most types of human cancers.[10–12] We have previously shown that microRNA expression is associated with prognosis in patients with lung,[13,14] colon,[15] gastric[16] and esophageal cancer.[17,18] Specifically for CC, we have shown that patients with tumors expressing high levels of an oncogenic microRNA, miR-^{21}, have a worse prognosis for stage II or stage III colon cancer, demonstrating its potential as a prognostic indicator for colon cancer.[15] Consistent results have also been observed in other malignancies with increased expression of miR-^{21} being associated with a worse prognosis and/or therapeutic outcome in multiple cancers including lung cancer,[13,14,19] colon cancer,[15,20–22] pancreatic cancer,[23,24] breast cancer,[25,26] head and neck cancer,[27] tongue cancer,[28] astrocytomas[29] and chronic lymphocytic leukemia.[30] These data support the hypothesis that expression of miR-21 has potential as a prognostic indicator for a wide variety of malignancies. In most of these reports, miR-21 expression was measured from freshly-frozen tissues and the utility of measuring miR-21 expression from FFPE samples still remains unclear. For clinical application, it will be useful if miR-21 can be accurately measured from FFPE tissue and if its expression can stratify patients into risk groups. *In situ* hybridization of miR-21on FFPE colon cancer tissues has been used to stratify patients into low and high risk groups for survival,[22] but qRT-PCR measurements was not performed and the association between miR-^{21} and therapeutic outcome was not examined. Therefore, we determined if miR-^{21} expression from FFPE tissues was associated with cancer-specific mortality and therapeutic outcome for CC.

In the present study, we investigated the association of miR-^{21} expression, determined by qRT-PCR from FFPE samples, with prognosis of patients with CC. We also investigated the influence of hematoxylin contamination on qRT-PCR results.

Material and Methods

Patients and tissue samples

We used archival FFPE tissues from 301 patients who had undergone surgical excision of CC. Rectal cancer patients were excuded. Of 301 patients, 156 patients were treated at the Hiroshima University Hospital (Hiroshima, Japan) between 1997 and 2003, and 145 patients were treated at the Mainz University Clinic Center and its teaching hospitals in Germany between 2005 and 2007. Detailed background information including age, sex, TNM stage, tumor location, survival times from diagnosis, receipt of adjuvant chemotherapy (for patients with stage I-III CC), and receipt of postoperative chemotherapy (for patients with stage IV CC) has been collected. The final date of follow-up was December 31, 2008 for the Japanese cohort and March 25, 2013 for the German cohort. Tumor histopathology was classified according to the World Health Organization Classification of Tumors system. Tumors were staged according to the TNM classification system. This study was approved by the Institutional Review Board of the National Institutes of Health, the Ethical Committee for Human Genome Research of Hiroshima University (Hiroshima, Japan) and Landsaerztekammer Rheinland-Pfalz (Mainz, Germany).

RNA extraction

FFPE samples were sectioned (10 μm), deparaffinized, and stained with hematoxylin and eosin to ensure that the sectioned block contained tumor cells. For the Japanese cohort, adjacent sections were stained by hematoxylin and the tumor area was marked under a light microscope. For German cohort, the tumor areas in adjacent sections were marked under a light microscope without hematoxylin staining. Tumor areas were macrodissected with sterile disposable scalpels (Cincinnati Surgical Company, Cincinnati, OH) and subjected to RNA isolation using the PureLink FFPE Total RNA

Isolation Kit (Invitrogen, Carlsbad, CA) according to the manufacturer's instructions with small modifications. This included a 10-min centrifugation at maximum speed in an Eppendorf 5415C benchtop centrifuge after proteinase K digestion to remove trace hematoxylin from the sample. Total RNA was quantified using the NanoDrop ND-1000 spectrometer (NanoDrop, Wilmington, DE) and both OD 260/280 and OD 260/230 ratios utilized for quality control.

qRT-PCR

Expression levels of miR-21 and RNU48 were measured using Taqman MicroRNA Assays (Applied Biosystems) while blinded to clinical outcomes. cDNA was synthesized using microRNA-specific primers and a TaqMan MicroRNA Reverse Transcription Kit (Applied Biosystems, Austin, TX) according to the manufacturer's instructions. Briefly, 40 ng of RNA was reverse transcribed in a 20 μL reaction with gene specific RT probes. qPCR was performed using the 7900 HT-Fast real-time PCR system (Applied Biosystems). We used small nuclear RNA (RNU48) as an endogenous normalization control for miR-21. All assays were performed in triplicate. Relative expression quantitation of miR-21 was calculated with RQ manager 1.2 (Applied Biosystems).

MSI analysis

Genomic DNA was extracted from FFPE samples (10 μm) from individual patients. The tumor area was marked under a light microscope without hematoxylin staining. Tumor areas and adjacent non-neoplastic areas were macrodissected with sterile disposable scalpels (Cincinnati Surgical Company) and subjected to DNA extraction by a phenol-chloroform method with proteinase K digestion.[31] The five microsatellite markers that were recommended by a National Cancer Institute (NCI) workshop on MSI (BAT25, BAT26, D2S123, D5S346 and D17S250) were used to examine paired nonneoplastic and tumor DNA for MSI status. PCR and subsequent analyses using ABI 3130XL Genetic Analyzer (Applied Biosystems) were performed, and the shift of PCR products from tumor DNA was compared to that of DNA from corresponding nonneoplastic tissue. The size of each fluorescent PCR product was calculated using GeneMapper software (Applied Biosystems). According to the guidelines of the international workshop of NCI,[32] tumors were classified as MSI-H when at least two of the five markers displayed novel bands, MSI-L when additional alleles were found with 1 of the ^{5} markers, and MSS when all microsatellite markers showed identical patterns in both tumor and non-neoplastic tissues. MSI-H and MSI-L were considered as MSI. MSI status was scored independently by two examiners.

Statistical analysis

Univariable and multivariable Cox regression was used to evaluate the associations between clinical covariates and cancer-specific mortality in Stata 11 (College Station, TX). Hazard ratio (HR) and 95% confidence interval (CI) were estimated from Cox proportional hazard models. For all analyses, age was treated as a categorical variable (greater than or equal to 65-years old versus <65-years old). Multivariable Cox regression models were built using stepwise removal of variables with a threshold for removal at $p < 0.10$. Differences in miR-21 expression levels between two groups were tested by the Mann–Whitney U test using Graphpad Prism v5.0 (Graphpad Software, San Diego, CA). High miR-21 expression was defined on the basis of highest tertile for each cohort, similar to our previous publication on miR-21 in two independent patient cohorts from USA and Hong Kong.[15] Kaplan–Meier survival curves were constructed for high-miR-21 and low-miR-21 patients using Graphpad Prism v5.0. Differences between survival curves were tested for statistical significance by a Log-rank test. A p value of < 0.05 was considered statistically significant. Two sided p values are reported for all statistical tests.

Results

Expression of miR-21 in stages I-IV of CC (Japanese cohort)

We examined whether the expression of miR-21 in FFPE CC tissues was associated with cancer-specific mortality. While optimizing our RNA isolation techniques from FFPE tissue, we found that there were trace amounts of hematoxylin in several RNA preparations (Supporting Information Fig. S1) and that hematoxylin contamination in RNA preparations interferes with qRT-PCR (Supporting Information Fig. S2). An extra centrifugation step after proteinase K digestion was found to remove most of the hematoxylin (Supporting Information methods and Supporting Information Fig. S1). Therefore, all RNA samples were prepared in this manner.

qRT-PCR of miR-21 was performed in all samples of the Japanese cohort ($n = 156$, Table 1). We first investigated the association between miR-21 expression levels and clinicopathological characteristics (Supporting Information Fig. S3). Expression levels of miR-21 were significantly higher in T4 cases than T1, T2, and T3 cases ($p = 0.03$, 0.03 and 0.04, respectively; Mann–Whitney U test), indicating that elevated miR-21 expression was associated with a more aggressive histology of the primary tumor. Expression of miR-21 was also significantly elevated in node-positive cases (N1) compared to node-negative cases (N0, $p = 0.03$; Mann–Whitney U test). Expression levels of miR-21 were not associated with age, sex, M classification, or TNM stage.

Next, we evaluated the association between miR-21 expression levels and prognosis. When analyzing all cases regardless of stage, we found that cases with high miR-21 expression had slightly worse cancer-specific mortality although this did not achieve statistical significance ($p = 0.083$, Log-rank test, Supporting Information Fig. S4). Similar results were seen with multivariable Cox regression analyses (Supporting Information Table S1).

Stage I CC patients have very good survival prognosis and surgery is usually curative while stage IV CC patients have

Table 1. Characteristics of the study populations

	Japanese cohort (n = 156)	German cohort (n = 145)
Recruitment area	Hiroshima, Japan	Mainz, Germany
Age, mean (range), year	63 (29–89)	70 (39–90)
Sex, No. (%)		
Male	93 (60)	75 (52)
Female	63 (40)	70 (48)
Follow-up time, median (range), month	54.0 (2.8–111.8)	51.6 (1.2–72.4)
Adjuvant chemotherapy[1] (for stage I–III), No. (%)		
Received	59 (43)	25 (17)
Did not received	77 (57)	120 (83)
Postoperative chemotherapy[1] (for stage IV), No. (%)		
Received	17 (85)	0
Did not received	3 (15)	0
TNM stage, No. (%)		
I	49 (31)	0
II	40 (26)	145 (100)
III	47 (30)	0
IV	20 (13)	0
Tumor location, No. (%)		
Proximal	28 (18)	63 (43)
Distal	128 (82)	73 (50)
Not available	0 (0)	9 (6)
MSI status, No. (%)		
MSI	7 (11)	19 (15)
MSS	54 (89)	111 (85)
Not available	95	15

[1]Chemotherapy regimens were primarily 5-fluorouracil based regimens. Abbreviations: MSI, microsatellite instability; MSS, microsatellite stable.

dismal prognoses with 5-year survival rates below 10%. The survival of patients with stage II or stage III CC are intermediate and it is these patients that would benefit the most from prognostic biomarkers. Therefore, we restricted our analysis of the prognostic value of miR-21 to patients with stage II and stage III CC (n = 87). We found that cases with high miR-21 expression had significantly worse cancer-specific mortality than those with low miR-21 expression (p = 0.0008, Log-rank test, Fig. 1*a*). Both univariable and variable Cox proportional hazards analysis were used to further evaluate the association of miR-21expression with cancer-specific mortality (Table 2). In univariable analysis, high expression of miR-21 (HR, 4.17; 95% CI, 1.64–10.11; p = 0.003), receipt of adjuvant chemotherapy (HR, 0.38; 95% CI, 0.16–0.94; p = 0.037) and T classification (HR, 4.23; 95%CI, 1.81–10.11; p = 0.001) were significantly associated with survival while TNM stage (HR, 1.59; 95% CI, 0.63–4.05; p = 0.329), age (HR, 2.05; 95% CI, 0.81–5.21; p = 0.132), tumor location (HR, 0.73; 95% CI, 0.24–2.21; p = 0.582) and sex (HR, 1.12; 95% CI, 0.45–2.78; p = 0.805) were not. In the final multivariable model, miR-21 expression was an independent prognostic classifier (HR, 3.13; 95% CI, 1.20–8.17; p = 0.019).

Expression of miR-21 in an independent patients with stage II CC (German cohort)

We next evaluated the expression of miR-21 in an independent German cohort of stage II CC patients (n = 152). On the basis of our observation that that hematoxylin staining could affect qRT-PCR, we extracted RNA from the FFPE sections of the German cohort without hematoxylin staining. Although we did not stain FFPE samples with hematoxylin, the tumor area could be marked in the FFPE sections under a light microscope because the tumor/nontumor borderline was clearly identified in the stage II tumors. After total RNA was extracted from all samples of the German cohort, seven samples were excluded with OD 260/230 ratios <1.00. For the remaining 145 samples (OD 260/230 ratio ranged from 1.07 to 2.04; mean, 1.65) qRT-PCR was performed.

The association between miR-21 expression levels and clinico-pathological characteristics was analyzed (Supporting Information Fig. S3). Expression levels of miR-21 were not associated with age, sex or T classification. Next, association between miR-21 expression levels and patient survival was investigated by Kaplan–Meier analysis. We found that high miR-21 expression was significantly associated with increased cancer-specific mortality (p = 0.047, Log-rank test, Fig. 1*c*). Because adjuvant chemotherapy for patients with stage II CC influences patients' survival, we analyzed individuals who did not receive adjuvant chemotherapy. We found that high miR-21 expression was associated with increased cancer-specific mortality in that group (p = 0.040, Log-rank test, Fig. 1*d*).

Univariable and multivariable Cox proportional hazards analysis was used to further evaluate the association of miR-21expression with survival to evaluate the potential for miR-21 expression as a prognostic biomarker (Table 3). In univariable analysis, high expression of miR-21 (HR, 2.65; 95% CI, 0.98–5.95; p = 0.055) and T classification (HR, 2.67; 95% CI, 0.96–7.41; p = 0.060) were marginally associated with survival while tumor location, age, sex or adjuvant chemotherapy were not. In the final multivariable models, which included miR-21 expression and T classification and tumor location, high miR-21 expression was an independent prognostic indicator (HR, 2.65; 95% CI, 1.06–6.66; p = 0.037). These results demonstrate that miR-21 may be a useful biomarker to identify TNM stage II patients with high risk of recurrence.